



A global perspective on Last Glacial Maximum to Holocene climate change

Jeremy D. Shakun^{a,*}, Anders E. Carlson^{b,1}

^a Department of Geosciences, Oregon State University, Corvallis, OR 97331, USA

^b Department of Geoscience, University of Wisconsin, Madison, WI 53706, USA

ARTICLE INFO

Article history:

Received 11 April 2009

Received in revised form

20 March 2010

Accepted 28 March 2010

ABSTRACT

While the abrupt climate events of the last deglaciation are well defined in ice core records from the polar regions of both hemispheres, their manifestation elsewhere is less well constrained. Here we compile 104 high-resolution paleoclimate records to characterize the timing and spatial pattern of climate change during the last deglaciation. This compilation indicates relatively concurrent timing of the Last Glacial Maximum (LGM; peak glacial conditions) and the Altithermal (peak interglacial conditions) in the Northern (22.1 ± 4.3 ka and 8.0 ± 3.2 ka) and Southern (22.3 ± 3.6 ka and 7.4 ± 3.7 ka) Hemispheres, suggesting the hemispheres were synchronized by greenhouse gases, local insolation, and/or Northern Hemisphere induced ocean circulation changes. The magnitude of the glacial–interglacial temperature change increases with latitude, reflecting the polar amplification of climate change, with a likely minimum global mean cooling of ~ -4.9 °C during the LGM relative to the Altithermal.

Empirical orthogonal function (EOF) analysis of 71 records spanning 19–11 ka indicates that two modes explain 72% of deglacial climate variability. EOF1 (61% of variance) shows a globally near-uniform pattern, with its principal component (PC1) strongly correlated with changes in atmospheric CO₂. EOF2 (11% of variance) exhibits a bipolar seesaw pattern between the hemispheres, with its principal component (PC2) resembling changes in Atlantic meridional overturning circulation strength. EOF analysis of 90 records from 15 to 11 ka indicates that northern and southern modes of climate variability characterize the Younger Dryas–Bølling/Allerød interval. These modes dominate at the higher latitudes of each hemisphere and exhibit a complex interaction in the tropics. The magnitude of the Younger Dryas climate anomaly (cooler/drier) increases with latitude in the Northern Hemisphere, with an opposite pattern (warmer/wetter) in the Southern Hemisphere reflecting a general bipolar seesaw climate response. Global mean temperature decreased by ~ 0.6 °C during the Younger Dryas. Therefore, our analysis supports the paradigm that while the Younger Dryas was a period of global climate change, it was not a major global cooling event but rather a manifestation of the bipolar seesaw driven by a reduction in Atlantic meridional overturning circulation strength.

© 2010 Elsevier Ltd. All rights reserved.

1. Introduction

The development over the past decade of many higher resolution paleoclimate records spanning the last deglaciation provides an unprecedented perspective on orbital and millennial-scale climate changes during this time period (Clement and Peterson, 2008). Nevertheless, vast areas of the planet that may be integral players in any given climate event remain undersampled. Moreover, there is a danger in relying on a few records to characterize hemispheric to global climate change. This is particularly evident when attempting

to determine the spatial response of the climate system to the millennial-scale events of the last deglaciation.

The most prominent deglacial events of the Northern Hemisphere are Heinrich Event 1 (H1, ~ 17.5 to 16 ka) and the associated Oldest Dryas cold period (~ 18 to 14.7 ka), the Bølling/Allerød warm period (~ 14.7 to 12.9 ka) and the Younger Dryas cold event (~ 12.9 to 11.7 ka) (Fig. 1) (Alley and Clark, 1999). In the Southern Hemisphere, the most noted deglacial event is the Antarctic Cold Reversal, which was originally defined in Antarctic ice cores as cooling or cessation of deglacial warming ~ 15 to 13 ka (Fig. 1) (Jouzel et al., 1995). Proxy records suggest a so-called bipolar seesaw response during this deglacial interval, with antiphased temperature anomalies in the two polar hemispheres (Broecker, 1998; Alley and Clark, 1999; Blunier and Brook, 2001; Clark et al., 2002). Concurrent changes in Atlantic meridional overturning circulation (AMOC) strength in response to North Atlantic surface freshening may have

* Corresponding author. Tel.: +1 541 737 1248.

E-mail addresses: shakunj@geo.oregonstate.edu (J.D. Shakun), acarlson@geology.wisc.edu (A.E. Carlson).

¹ Tel.: +1 608 262 1921.

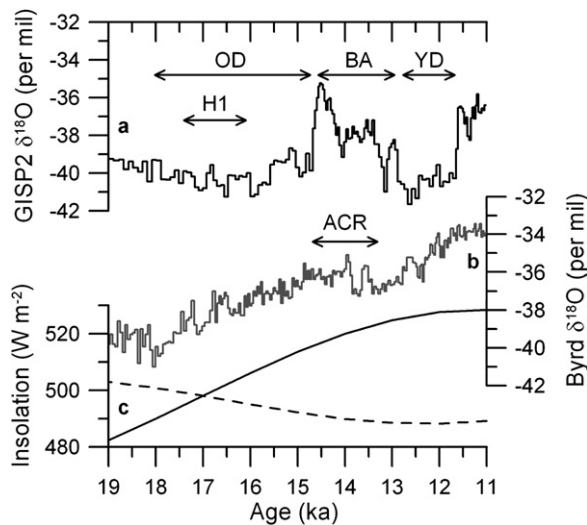


Fig. 1. Deglacial ice core time series and insolation. (a) GISP2 $\delta^{18}\text{O}$ (black step plot) (Blunier and Brook, 2001). (b) Byrd $\delta^{18}\text{O}$ (grey step plot) (Blunier and Brook, 2001). (c) Insolation for 60°N on June 21 (black line) and for 60°S on December 21 (dashed black line) (Berger and Loutre, 1991). The timing of the Younger Dryas (YD), Bølling/Allerød (B/A), Heinrich Event 1 (H1), Oldest Dryas (OD) and Antarctic Cold Reversal (ACR) are denoted.

redistributed heat and thus caused this bipolar seesaw behavior (Boyle and Keigwin, 1987; Broecker, 1998; Clark et al., 2002; McManus et al., 2004; Robinson et al., 2005; Stouffer et al., 2006; Carlson et al., 2007a; ; Liu et al., 2009). In contrast, arguments for global cooling during the Younger Dryas and Oldest Dryas, predominately based on Southern Hemisphere valley glacier records, would imply an atmospheric forcing mechanism rather than variability in AMOC strength (Huesner and Rabassa, 1987; Denton and Hendy, 1994; Lowell et al., 1995; Ariztegui et al., 1997; Denton et al., 1999a; ; Ivy-Ochs et al., 1999; Broecker, 2003; Moreno et al., 2001). These differing views on the impact of the Younger Dryas and Oldest Dryas thus imply profoundly different drivers of abrupt climate change (Clement and Peterson, 2008).

A more complete and accurate characterization of past climate events requires the integration of a large body of records, with sufficient resolution and dating control to adequately constrain the nature and behavior of different parts/regions of the climate system during an event. Here we compile 104 deglacial paleoclimate records to quantify the timing of the Last Glacial Maximum (LGM) and Holocene Altithermal, and perform time series analyses to identify patterns in deglacial climate variability, focusing on the Bølling/Allerød–Younger Dryas period. Our analyses indicate an interhemispheric synchronicity in the timing of the LGM and Altithermal. Similar to previous work with a smaller number of records (Clark et al., 2002), Empirical Orthogonal Function (EOF) analysis identifies two major modes of deglacial climate variability: a global pattern paralleling changes in atmospheric CO_2 concentration and a bipolar pattern resembling variations in AMOC strength. The Younger Dryas, as documented in 90 records, confirms this bipolar pattern with climate deterioration focused in northern high latitudes and climate amelioration in the Southern Hemisphere. We find that global cooling during the Younger Dryas was $\sim 1/10$ of LGM cooling.

2. Empirical orthogonal function methodology

The database generated in this study is comprised of many of the highest-resolution and best-dated climate records currently

available that cover the last 25 kyr (Supplementary Data, Fig. 2). We do not assign special consideration to the particular characteristics (e.g., geographic location, type of proxy, density of radiocarbon ages) of the climate records in forming the database, but rather simply attempt to include as many records as possible that are of sufficient temporal resolution to provide meaningful information on deglacial climate changes. Fig. 3 shows the resolution of the records; the median resolution is 130 years from 19 to 11 ka and 106 years from 15 to 11 ka. Approximately 80% of the records have resolutions higher than 250 years, corresponding to, for example, at least five data points during the Younger Dryas interval. The records are biased toward ocean margins due to the relative paucity of high-resolution time series from land as well as low sedimentation rates and carbonate dissolution in the deep ocean.

We use EOF analysis to compute objectively defined modes of variability from this database. EOF analysis identifies spatial-temporal patterns of variability in a dataset through a linear decomposition of the records into a series of independent basis functions (Mix et al., 1986a,b). The EOFs are the eigenvectors of the temporal correlation matrix, which, as opposed to the covariance matrix, results in each dataset providing equal weight toward the EOFs. Such an approach is necessary because this database is comprised of many different proxies, which have different variances in their respective units and are thus not directly comparable.

Records were linearly interpolated to 100 yr resolution. Results are unaffected by factor-of-two changes in interpolated resolution. We find that the principal components (PCs) are relatively insensitive to the number of input records used through a jack-knifing method in which 10, 20, 30, ...90% of the records were randomly removed 100 times and the PCs recalculated. Monte Carlo simulations introducing random age model errors to the input records suggest the chronologies of the PCs are also relatively robust as these errors tend to be “averaged out” in the EOF analysis. Published chronologies were used for each record. Radiocarbon chronologies were calibrated when necessary. The chronologies were referenced to years before 1950 AD if the original author defined the “present” and left unchanged from the published version if not. Records were oriented so that “warm”/“wet” points upwards.

3. The Last Glacial–interglacial transition

3.1. Timing of the Last Glacial maximum–altithermal

We define the LGM (Altithermal) as the age of the lowest (highest) value in the 1 kyr running mean of the time series (Supplementary Data). A 1 kyr average was used in order to identify robust, persistent climate states and avoid anomalous outlying values. We use 56 records that cover at least 24–11 ka for the LGM and 78 records covering at least 10–2 ka for the Altithermal. Note that our use of existing terminology – ‘LGM’ and ‘Altithermal’ – for the most extreme climate periods is merely for convenience and not meant to imply our definition of these climate states is necessarily relevant to other definitions (e.g., maximum ice volume, sea-level lowstand, etc.).

There is considerable variation in the timing of these extreme climate states in different records with the LGM and Altithermal each spread over more than 10 kyr (Fig. 4). Nevertheless, the timing of the LGM and Altithermal in the Northern (22.1 ± 4.3 ka, 8.0 ± 3.2 ka) and Southern (22.3 ± 3.6 ka, 7.4 ± 3.7 ka) Hemispheres is statistically indistinguishable and their mean ages differ by only a few centuries (Fig. 4). Note that there is no latitudinal trend in the timing of the LGM ($r^2 = 0.0036$, $p = 0.66$) or Altithermal ($r^2 = 0.0085$, $p = 0.43$). These values are nearly unchanged when considering only the proxy temperature records.

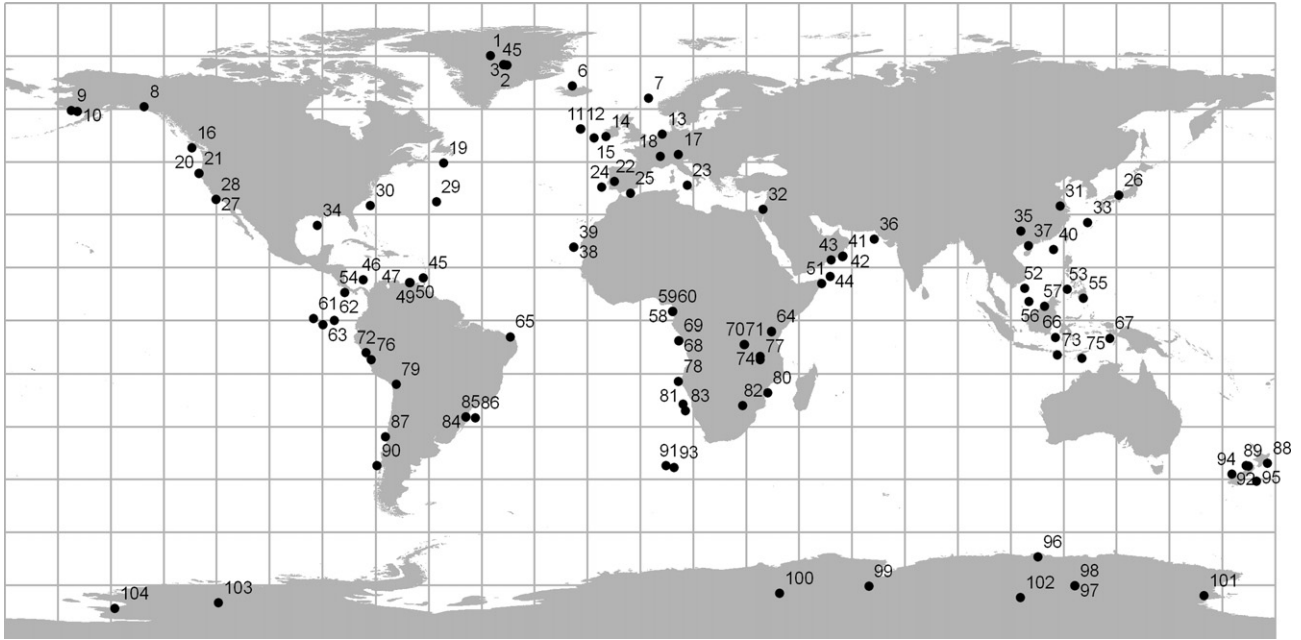


Fig. 2. Map of the time series utilized in this manuscript on a 15° grid. See Supplementary Data for specific time series locations and descriptions.

3.2. Magnitude of the glacial–interglacial temperature change

Using just the proxy records of temperature (44 records), we calculate the glacial–interglacial temperature change at each site by taking the difference between the mean values during the global LGM (22.2 ± 4.0 ka) and Altithermal (7.8 ± 3.4 ka) (Supplementary Data). Note that not all records span these entire 1σ time intervals, but a mean value was still calculated from the data that lie within them. Glacial–interglacial temperature increases range from 0.4 to 17 °C (Fig. 5). The magnitude of temperature changes increases poleward in both hemispheres, with significantly greater cooling in the northern relative to the southern high latitudes. However, the

northern high latitudes are represented by only one point (GISP2 ice core) making this latter conclusion tenuous. At the same time, the GISP2 site has experienced relatively small changes in albedo and elevation since the LGM (Cuffey and Clow, 1997), so it is conceivable that northern high latitude regions formerly covered by sea ice or ice sheets cooled as much or more than GISP2 at the LGM. Nevertheless, there is a clear need for more high-resolution deglacial temperature records in the northern high latitudes.

We calculate a net global LGM cooling relative to the Altithermal with these data by fitting a 3rd order polynomial to the glacial–interglacial temperature changes as a function of latitude ($r^2 = 0.80$, $p < 0.0001$) and then weighting by latitudinal area. The

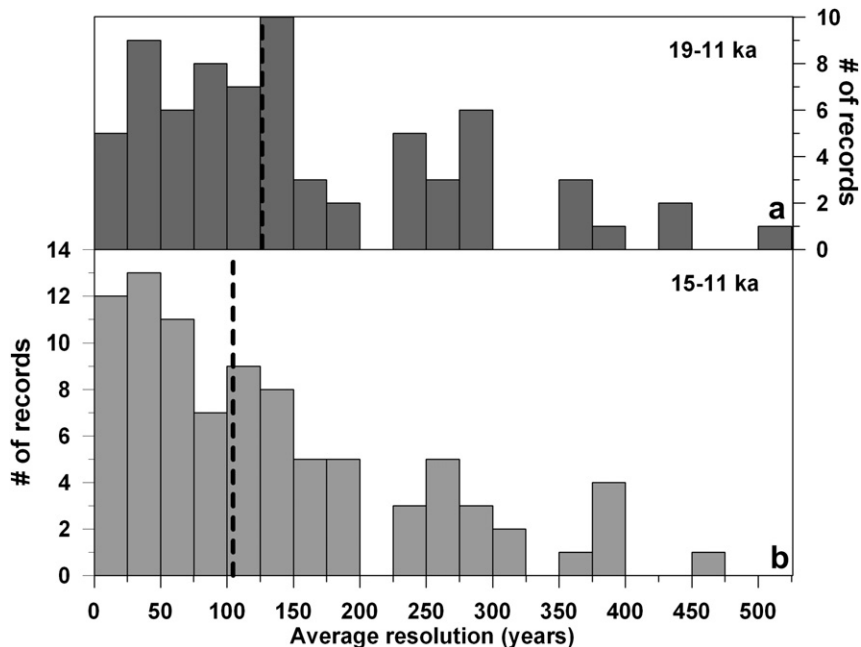


Fig. 3. Histograms of the average resolution of the climate records used in this study over the intervals (a) 19–11 ka and (b) 15–11 ka. The vertical dashed lines show the median resolution of the records.

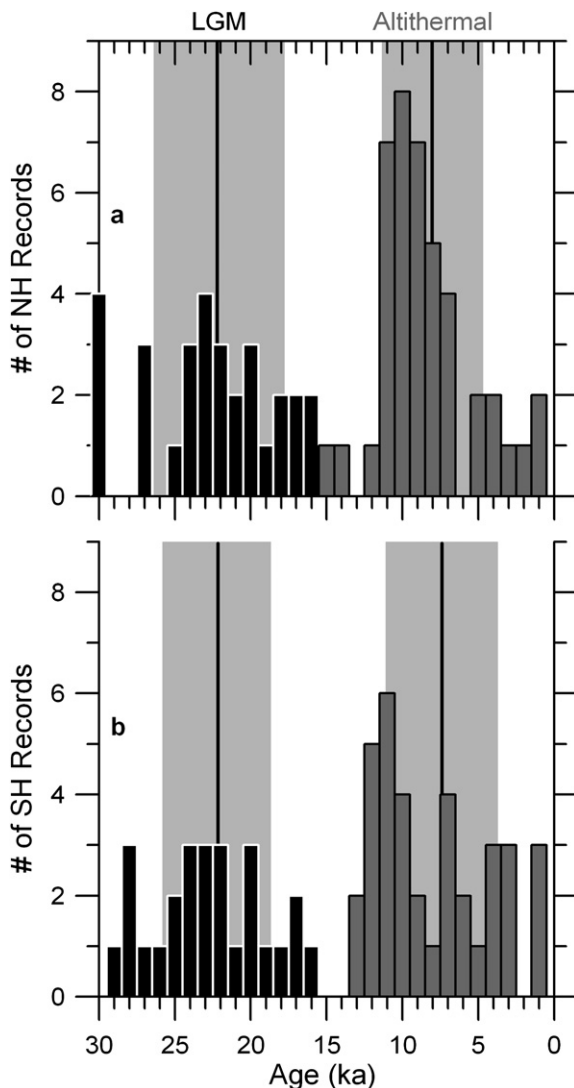


Fig. 4. Timing of the LGM and Altithermal for the Northern (a) and Southern Hemispheres (b). Bins are 1 kyr. Black line and gray box denote the average and standard deviation of LGM and Altithermal timing for each hemisphere. Northern Hemisphere LGM = 22.1 ± 4.3 ka; Southern Hemisphere LGM = 22.3 ± 3.6 ka; Northern Hemisphere Altithermal = 8.0 ± 3.2 ka; Southern Hemisphere Altithermal = 7.4 ± 3.7 ka.

resulting global cooling at the LGM is ~ 4.9 °C, which should likely be considered a minimum estimate for several reasons. Most of the records used are from the oceans, which are less sensitive to climate change than the continents in climate models (e.g., Pinot et al., 1999; Otto-Bliesner et al., 2006). Furthermore, sea level lowering during the LGM effectively raised the continents by ~ 120 m (e.g., Clark and Mix, 2002), which would have resulted in an additional ~ 0.75 °C adiabatic cooling of marine air advected over land areas. Finally, proxy temperature records are absent from areas formerly covered by sea ice and ice sheets. These areas likely experienced the greatest cooling during the LGM due to their greatly altered albedo, and, in the case of the ice sheets, increased elevation. It should also be cautioned that our estimate for LGM cooling is limited by its relatively small sample size.

3.3. EOF Analysis of deglacial climate variability

EOFs were computed for the last deglaciation (19–11 ka) using 71 records (Supplementary Data). EOF1 dominates the variance in these datasets (61% of total) and shows strong positive factor loadings in

nearly every record (Fig. 6b), similar to the results of Clark et al. (2002). PC1 rises exponentially over this interval, although this pattern is interrupted by a plateau from ~ 14.5 to 12.5 ka. Rising boreal summer insolation as well as decreasing global ice volume could potentially explain the deglacial trend seen in PC1 (Fig. 7). However, these forcings likely had little effect on Southern Hemisphere climate (Manabe and Broccoli, 1985; Broccoli, 2000), and Southern Hemisphere records have equally high EOF1 loadings as those in the Northern Hemisphere. The largest deglacial climate forcing (or feedback) common to both hemispheres is the increase in atmospheric greenhouse gas concentration, particularly CO₂. The plateau in PC1 ~ 14.5 to 12.5 ka resembles the plateau in atmospheric CO₂ during this same time interval and not insolation or ice volume (Fig. 7). Indeed, PC1 is notably similar to CO₂ over its entire length ($r^2 = 0.97$ with Dome C; $r^2 = 0.88$ with Siple Dome; $r^2 = 0.88$ with Dome F; $p < 0.0001$ for all 3 comparisons) (Monnin et al., 2001; Ahn et al., 2004; Kawamura et al., 2007). Note that these CO₂ records were not used in this analysis and thus did not contribute to PC1.

EOF2 explains 11% of the variance in the database with a more complex factor loading pattern than EOF1 (Fig. 6c). Generally negative loadings in the Southern Hemisphere and positive loadings in the Northern Hemisphere suggest EOF2 records a bipolar seesaw response, similar to the results of Clark et al. (2002). Tropical and subtropical loading signs are quite variable in both hemispheres. PC2 decreases from ~ 19 to 16 ka, with an abrupt increase ~ 14.7 ka, followed by a second decrease ~ 12.9 ka and increase ~ 11.6 ka (Fig. 8). Comparison with a Pa/Th proxy record of AMOC strength (McManus et al., 2004) (not included in the analysis) shows significant commonality (Fig. 8) ($r^2 = 0.55$, $p < 0.0001$).

Higher order EOFs account for little variance ($< 7\%$) in the database and do not show spatially coherent patterns. We therefore consider them insignificant and do not discuss them further.

4. Bølling/Allerød–Younger Dryas climate variability

4.1. EOF analysis of climate during the Bølling/Allerød–Younger Dryas

Most of the climate variability from 19 to 11 ka is associated with the overall deglacial trend with relatively little variance at millennial time scales. Therefore, we focus the EOF analysis to 15–11 ka using 90 records to better characterize climate variability during the Bølling/Allerød–Younger Dryas oscillations (Supplementary Data). Over half of the variance in this database can be explained by two modes of variability of nearly equal significance; EOF1 explains 32% and EOF2 explains 26% of the variance (Fig. 9). The jackknifing results indicate these modes are robust (Fig. 10). EOFs 3 and 4 account for only 12 and 5% of the variance with no pattern in their loadings and are thus considered insignificant.

The first two EOFs display what are to a first order opposite spatial patterns (Fig. 9). EOF1 has large positive loadings in the extratropical Southern Hemisphere, which become progressively smaller and of mixed sign in the tropics and Northern Hemisphere (Fig. 9b). EOF2 displays large positive loadings in the Northern Hemisphere and increasingly smaller and mixed signed loadings in the tropics and Southern Hemisphere (Fig. 9c). Thus, EOF1 and EOF2 can be described as representing “southern” and “northern” modes of variability, similar to the results of an EOF analysis of Marine Isotope Stage 3 records (Clark et al., 2007). Interestingly, some low latitude records have intermediate to large loadings for EOF1 and/or EOF2 suggesting that tropical climate cannot be adequately explained without both EOFs. PC1 increases gradually from ~ 14.9 to 13.8 ka, is relatively constant from ~ 13.8 to 13.0 ka and increases again more strongly after ~ 13.0 ka (Fig. 10a). PC2

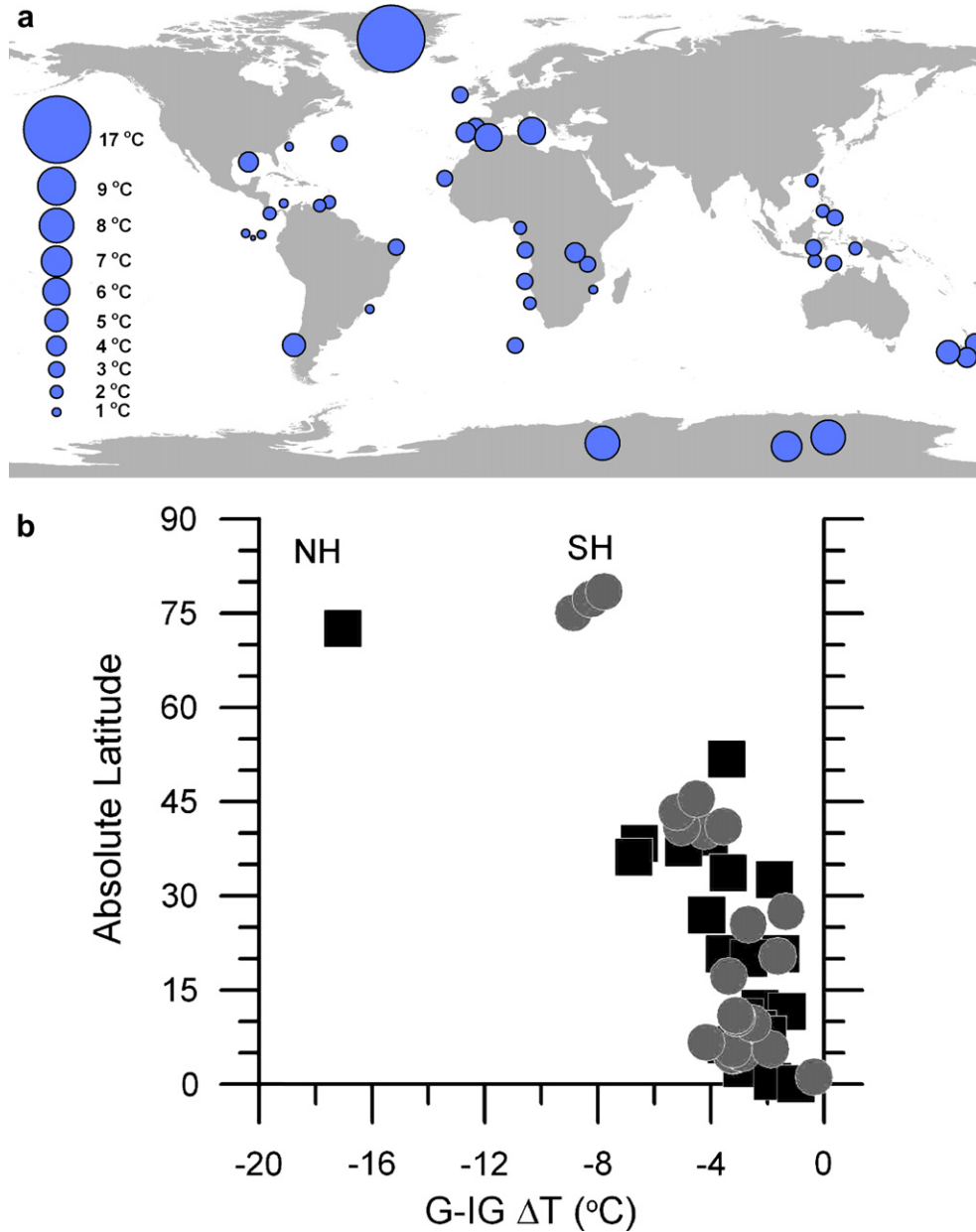


Fig. 5. Magnitude of the glacial-interglacial temperature change relative to absolute latitude. Black squares are the Northern Hemisphere (NH), gray circles the Southern Hemisphere (SH).

shows three major transitions, with increases at ~14.6 and 11.7 ka separated by a decrease at ~13.0 ka (Fig. 10b).

Dividing the records by region and recalculating the 15–11 ka EOFs helps to quantify the influence of these northern and southern modes around the world. EOFs were computed separately for records from the extratropical Northern Hemisphere (>30°N, $n = 25$), tropics (30°N–30°S, $n = 47$), and extratropical Southern Hemisphere (>30°S, $n = 18$). EOF1 accounts for substantially more variance than EOF2 in both the northern (41 and 19%) and southern (60 and 14%) extratropics, but EOF1 and EOF2 are nearly equal in the tropics (29 and 25%). PC1 and PC2 for the tropics are quite similar to the first PCs for the southern ($r^2 = 0.88$, $p < 0.0001$) and northern ($r^2 = 0.88$, $p < 0.0001$) extratropics, respectively. Thus, there appear to be signals associated with the higher latitudes of each hemisphere that exerted similar sized influences on the lower latitudes. Northern extratropical PC1 shares similarities with the Pa/Th record of AMOC

strength ($r^2 = 0.46$, $p = 0.004$) (McManus et al., 2004) while southern extratropical PC1 resembles atmospheric CO₂ ($r^2 = 0.85$, $p < 0.0001$) (Monnin et al., 2001). The northern mode, therefore, likely reflects the direct effects of AMOC variations, while the southern mode reflects greenhouse gas forcing and the processes affecting it such as changes in Southern Ocean circulation, sea ice extent and upwelling, which may have been forced in turn by AMOC variability (Monnin et al., 2001; Ahn and Brook, 2008; Barker et al., 2009).

Further separating the tropical records into those that are proxies for temperature ($n = 33$) and precipitation/windiness ($n = 14$) and again calculating 15–11 ka EOFs reveals differences in how the high latitudes of the two hemispheres affected low latitude climate. The tropical temperature PC1 and PC2 account for 34 and 18% of the variance, and are again similar to PC1 for the southern ($r^2 = 0.93$, $p < 0.0001$) and northern ($r^2 = 0.86$, $p < 0.0001$) extratropics,

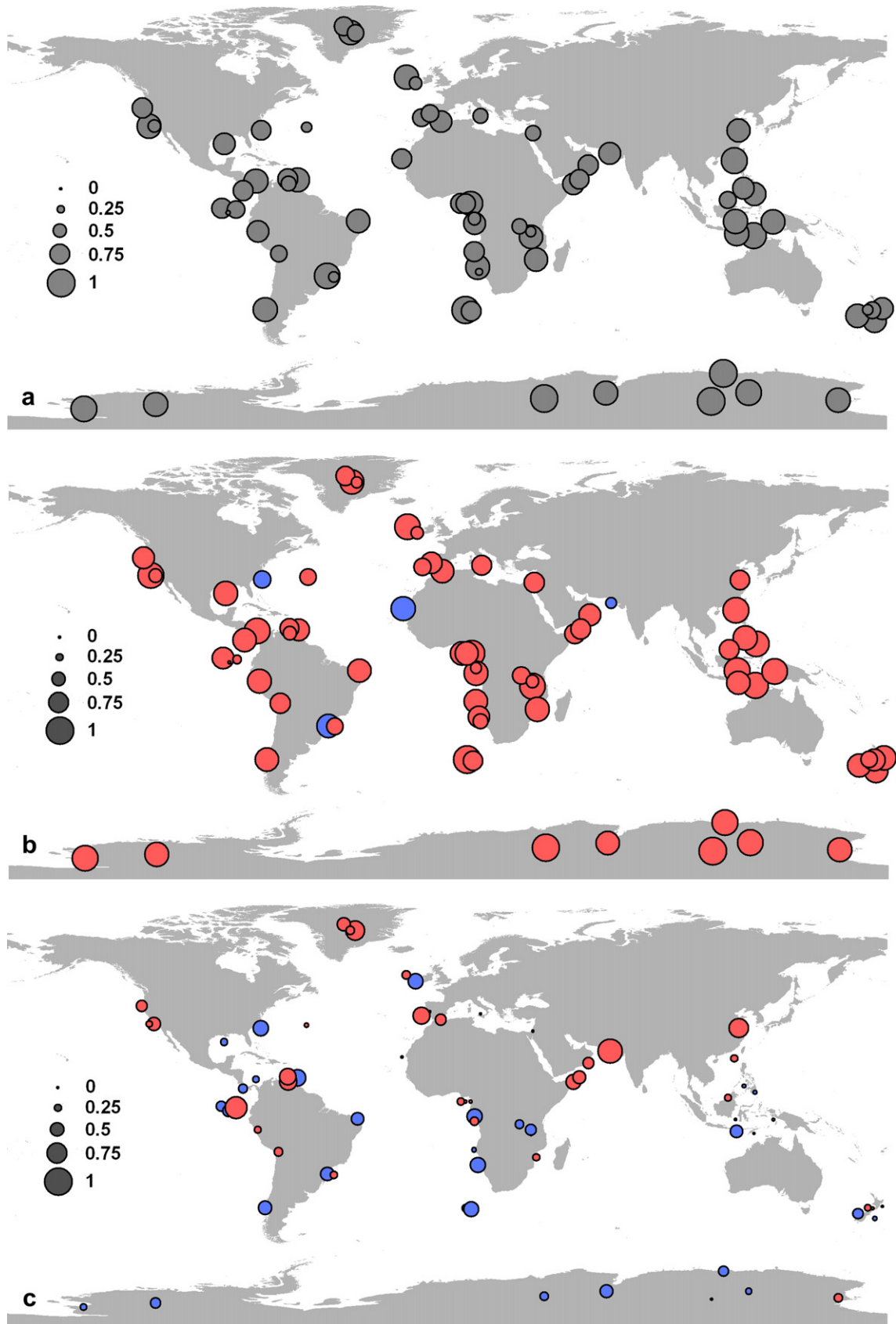


Fig. 6. Communality (a), EOF1 (b), and EOF2 (c) maps for the 19–11 ka analysis. EOF1 explains 61% of the deglacial variability; EOF2 explains 11% of the deglacial variability. Magnitude of each record's loading indicated by legend. Positive loadings are shown in red, negative loadings in blue. The square of the factor loading gives the fraction of variance in each record explained by the EOF. Communalities give the fraction of variance explained by the first two EOFs for each record. (For interpretation of the references to colour in this figure legend, the reader is referred to the web version of this article.)

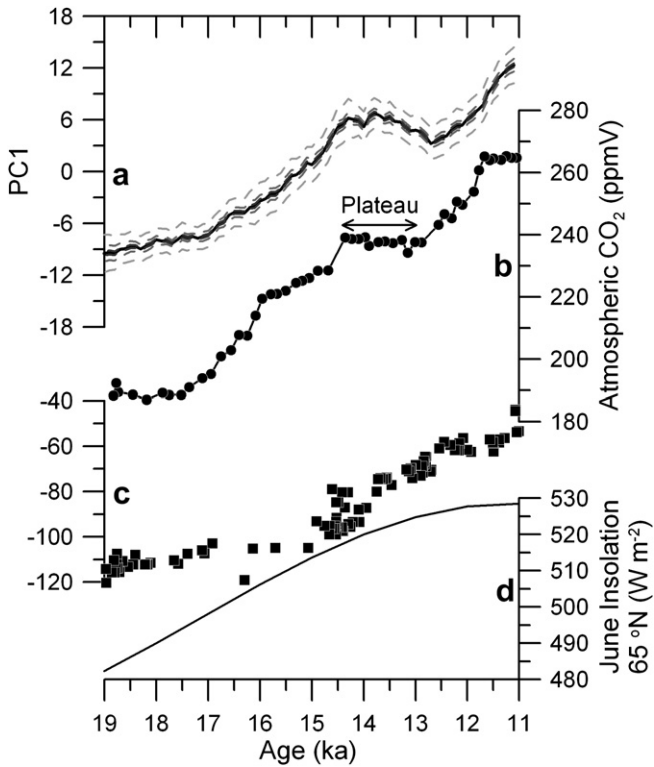


Fig. 7. 19–11 ka PC1 (a) and deglacial time series. Deglacial atmospheric CO₂ on EDC2 timescale (Monnin et al., 2001) (b). Boreal summer insolation (Berger and Loutre, 1991) (c). Deglacial relative sea level rise (Clark and Mix, 2002) (d). The plateau in atmospheric CO₂ is denoted. The dashed gray line confidence intervals around the PC give the standard deviation of 100 EOF calculations performed after randomly removing 10, 50 and 90% (in progressively lighter shades of gray) of the records during the jackknifing procedure described in Section 2.

respectively. The tropical precipitation/windiness PC1 and PC2 explain 47% and 16% of the variance, and are similar to PC1 for the northern ($r^2 = 0.79, p < 0.0001$) and southern extratropics ($r^2 = 0.68, p < 0.0001$), respectively. These results indicate that the northern

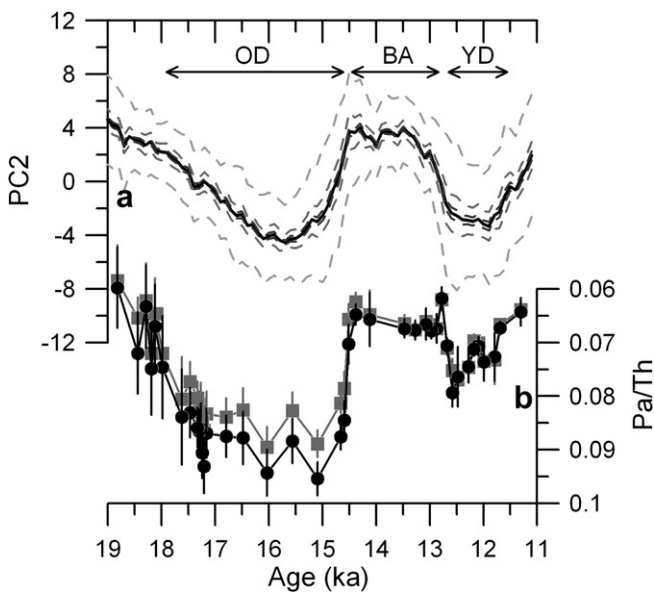


Fig. 8. 19–11 ka PC2 (a) and North Atlantic Pa/Th, a proxy for AMOC strength (McManus et al., 2004) (b). The timing of the Younger Dryas (YD), Bölling/Allerød (B/A) and Oldest Dryas (OD) are denoted. Gray confidence intervals show the results of the jackknifing procedure described in Section 2 and are the same as in Fig. 7.

mode of AMOC-driven climate variability had a larger impact on tropical atmospheric circulation and hydrology, likely caused by meridional displacements of the Intertropical Convergence Zone (ITCZ) (Chiang and Bitz, 2005; Yancheva et al., 2007). In contrast, tropical temperature appears to have been driven more strongly by the southern mode involving Southern Ocean processes and greenhouse gas forcing.

4.2. Relative magnitude of the Younger Dryas

The magnitude of the Younger Dryas around the planet has been used as a fingerprinting technique to identify the forcing locus (Broecker, 1994, 2003; Peteet, 1995). The differing nature of proxy records (e.g., $\delta^{18}\text{O}$ value versus Mg/Ca ratio versus sediment color), however, makes it difficult to relate the magnitude of the Younger Dryas in one record to another. The shift from a glacial to interglacial state provides a common backdrop against which to compare shorter events like the Younger Dryas. That is, the magnitude of the Younger Dryas can be determined as a fraction of the glacial-interglacial range in each record. While the glacial-interglacial range certainly varied around the globe (Fig. 5), particularly between the low and high latitudes, this method provides a first-order approach to mapping the size of the Younger Dryas. Here, we define the Younger Dryas interval in 72 records (Supplementary Data) in one of two ways: (1) in records where the Younger Dryas is distinct (e.g., Greenland ice cores, Cariaco Basin sediment, Hulu Cave speleothems) it is defined visually; (2) in records where the Younger Dryas is unclear or absent, the Greenland ice core Younger Dryas chronozone (12,850–11,650 years before 1950 AD) (Rasmussen et al., 2006) is used to define it. We compute a mean Younger Dryas value for the period 200 yr after the onset and 200 yr prior to the termination of the Younger Dryas interval. This 200 yr buffer is applied to ensure that only values from clearly within the Younger Dryas interval are used. The mean Younger Dryas value is then subtracted from the mean value for the interval 200–1000 yr preceding the Younger Dryas (approximately the Allerød). The difference between the Younger Dryas and Allerød is divided by the difference between the 1 kyr interval of highest (Altithermal) and lowest (LGM) values over the last 30 kyr. Therefore, Younger Dryas magnitudes range from -1 to $+1$, with larger absolute values reflecting larger Younger Dryas-age climate excursions. Positive numbers indicate a continuation of the overall deglacial trend during the Younger Dryas relative to the Allerød and negative numbers indicate a climate reversal.

Despite considerable spatial heterogeneity in the magnitude of the Younger Dryas, several patterns emerge from the map (Fig. 11). The spatial pattern is similar to 19–11 ka EOF2, with mainly negative values in the Northern Hemisphere and positive values in the Southern Hemisphere (Fig. 11a). As has long been known, the Younger Dryas was a return toward glacial conditions in many areas of the Northern Hemisphere, such as the mid to high latitudes and regions of the low latitudes affected by the ITCZ and monsoons. There is a slight latitudinal trend in the magnitude of the Younger Dryas, with a tendency for more negative values at higher Northern Hemisphere latitudes and more positive values at higher Southern Hemisphere latitudes (Fig. 11b). Low latitude Younger Dryas anomalies tend to be larger in precipitation-related proxies ($0.33 \pm 0.14, n = 10$) than temperature records ($0.13 \pm 0.16, n = 31$), suggesting that the Younger Dryas may have had a greater impact on the tropical hydrological cycle than on tropical sea surface temperatures.

4.3. Younger Dryas temperature anomalies

While normalizing the magnitude of the Younger Dryas by the glacial-interglacial range facilitates comparison of different types of

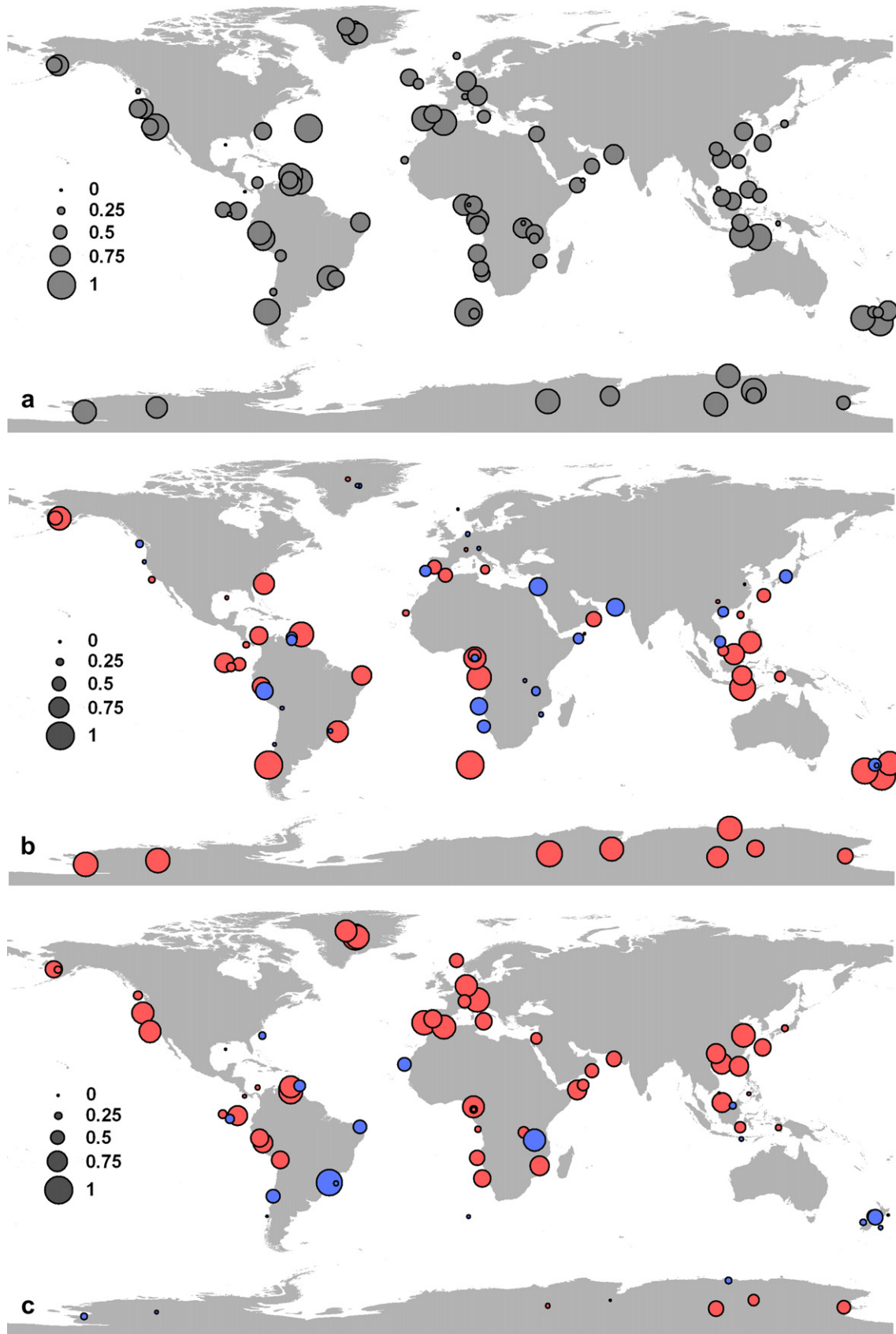


Fig. 9. Community (a), EOF1 (b), and EOF2 (c) maps for the 15–11 ka analysis. EOF1 and EOF2 explain 32% and 26% of the Bølling/Allerød–Younger Dryas variability, respectively. Magnitude of each record's loading indicated by legend. Positive loadings are shown in red, negative loadings in blue. (For interpretation of the references to colour in this figure legend, the reader is referred to the web version of this article.)

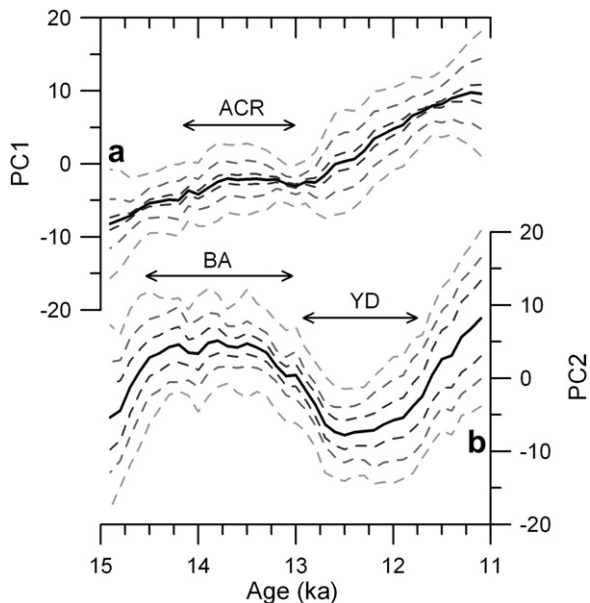


Fig. 10. Bølling/Allerød–Younger Dryas PCs from 15 to 11 ka; PC1 (a) and PC2 (b). The Younger Dryas (YD), Bølling/Allerød (B/A) and Antarctic Cold Reversal (ACR) are denoted. Gray confidence intervals show the results of the jackknifing procedure described in Section 2 and are the same as in Fig. 7.

proxy records, a more direct comparison can be made by focusing on calibrated temperature proxy records (55 records are included here; [Supplementary Data](#)). Note that these records do not provide a 1:1 comparison due to differences in proxies and calibrations (e.g., Mg/Ca, U^{k}_{37}) (Lea, 2003; Mix, 2006), as well as foraminifera depth habitats and seasonal biases. We compute mean Younger Dryas and Allerød temperatures using the same approach as described above for the magnitude of the Younger Dryas, and subtract to yield the Younger Dryas temperature anomaly relative to the preceding Allerød period.

The most striking feature of the temperature anomaly map and plot is the meridional gradient, particularly in the Northern Hemisphere (Fig. 12). Average cooling in the Northern Hemisphere high and mid latitudes is $\sim 5^{\circ}\text{C}$ ($n = 3$) and 2°C ($n = 13$), respectively. Tropical temperature anomalies are between 1 and -1°C , with the exception of Cariaco Basin (-3.3°C) (Lea et al., 2003), and average to nearly 0°C in both hemispheres ($n = 31$). The Southern Hemisphere mid to high latitude records show warming of 0 – 2°C ($n = 8$) with an average of $\sim 1^{\circ}\text{C}$. Anomalies greater than 2°C are concentrated around the North Atlantic region, near deepwater formation sites and their associated sea ice feedback.

To extrapolate the Younger Dryas temperature data globally, we use a similar technique as that employed with the glacial-interglacial change in temperature (Section 3.2.). We fit a 3rd order polynomial to the Younger Dryas temperature anomalies as a function of latitude ($r^2 = 0.50$, $p < 0.0001$) and weight by latitudinal area. The result is a global mean cooling of $\sim 0.6^{\circ}\text{C}$ during the Younger Dryas.

4.4. Relative magnitude of the Bølling/Allerød

We conduct an analysis similar to that presented above for the Younger Dryas (Section 4.2.) on the Bølling/Allerød to quantify its magnitude in relation to the glacial-interglacial range in each record (71 records; [Supplementary Data](#)). The mean value for the interval 16.0–15.0 ka is subtracted from the mean 14.5–13.5 ka value (\sim the Bølling/Allerød) and divided by the difference between the highest (Altithermal) and lowest (LGM) values in the 1 kyr running mean of

the time series. The results of this analysis are less clear than those for the Younger Dryas because the Bølling/Allerød was generally not a climate reversal and is therefore not as readily apparent against the overall deglaciation. Indeed, 82% of the records show positive anomalies for the magnitude of the Bølling/Allerød indicating a continuation of the deglacial trend (Fig. 13a). One notable result is a significant anticorrelation between the magnitudes of the Bølling/Allerød and Younger Dryas ($r^2 = 0.45$, $p < 0.0001$) (Fig. 13b). Records with large positive (negative) anomalies during the Bølling/Allerød tend to have large negative (positive) anomalies during the Younger Dryas. This relationship provides support for the notion that these events represent opposite responses of the climate system to the same fundamental forcing mechanism.

5. Discussion

The global average climate-defined LGM age of 22.2 ± 4.0 ka inferred from the 56 records analyzed here is broadly similar to both classical (CLIMAP, 1976–18 ^{14}C ka or ~ 21 ka) and more recent (Mix et al., 2001 – see below; Clark et al., 2009 – 26.5 to 19 ka) definitions of the LGM based on maximum global ice volume from foraminiferal $\delta^{18}\text{O}$ and/or sea level records. The LGM in 54% of the records fall within LGM Chronozone Level 2 (18–24 ka) and 39% are within LGM Chronozone Level 1 (19–23 ka) of Mix et al. (2001), suggesting that while these may be useful chronostratigraphic definitions of the LGM for the reasons presented by Mix et al. (2001), they do not appear to capture the length or variability of the LGM. It should be cautioned, however, that we identify the LGM in each record as a single point in time, which gives no indication of its duration or stability in any particular record; these would be worthwhile issues to investigate in the future. This similarity in timing between the climate and ice sheet-defined LGM intervals suggests a strong connection between maximum ice volume and glacial climate. Insofar as the onset of deglaciation immediately followed the minimum in a climate record (i.e., our LGM definition), our database indicates the deglaciation in most records began before the rise of CO_2 at ~ 17 to 18 ka (Monnin et al., 2001) and thus requires another forcing to have triggered deglaciation, even though CO_2 appears to have been a powerful feedback (see Section 3.3). Boreal summer insolation is the most likely candidate to explain the shift towards an interglacial ~ 22 ka, which implicates it as the ultimate forcing behind the termination of the LGM in the Northern Hemisphere (Barker et al., 2009; Clark et al., 2009). How, or if, this change in Northern Hemisphere energy impacted Southern Hemisphere climate is difficult to assess from our existing database (e.g., Clark et al., 2004, 2009; Huybers and Denton, 2008).

The similar timing of the LGM and Altithermal between the Northern and Southern Hemispheres (Fig. 4) suggests that the hemispheres were synchronized at orbital timescales. Atmospheric greenhouse gases are the most likely synchronizer given their global nature and strong forcing (Alley and Clark, 1999; Alley et al., 2002; Barrows et al., 2007a), which the 19–11 ka PC1 supports by showing global deglaciation tracked the rise in atmospheric CO_2 . However, as noted above, many of the climate records from both hemispheres begin their deglacial progression prior to the initial rise in CO_2 . Imbrie et al. (1993) and Gildor and Tziperman (2001) suggested that the effects of upwelled North Atlantic Deepwater on Southern Ocean temperatures may have also synchronized the hemispheres, but Alley and Clark (1999) argued that empirical evidence favors an out of phase response between the hemispheres due to changes in deepwater formation (Crowley, 1992). Alternatively, or additionally, both hemispheres may have responded to local insolation forcing, with a minimum in boreal summer intensity in the north and a minimum in austral summer length in the south leading to similar timing of the maximum glacial climate

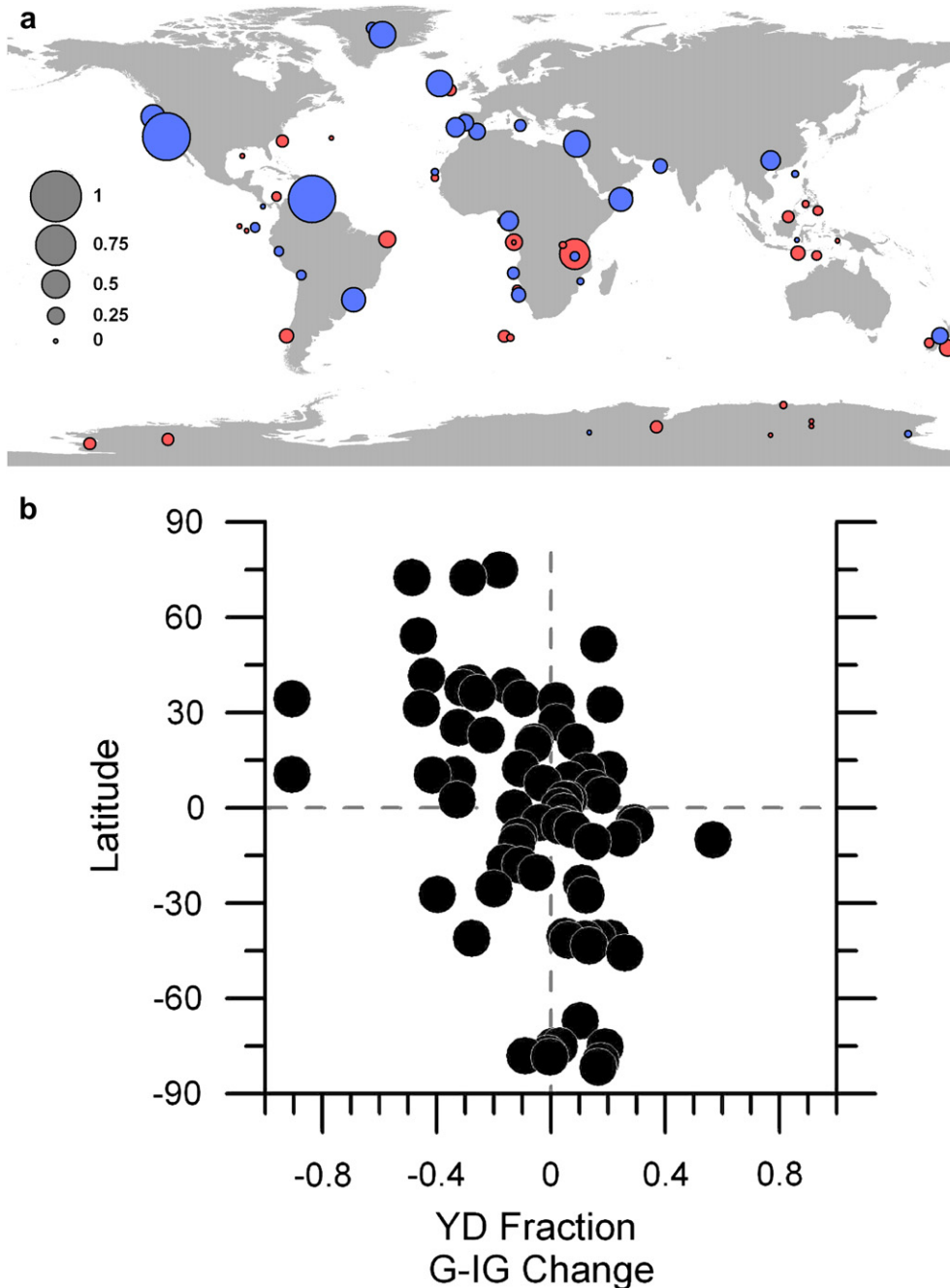


Fig. 11. Magnitude of Younger Dryas climate change. Map of the Younger Dryas fraction of the glacial-interglacial (G-IG) change (a). Red denotes Younger Dryas was continuation of deglacial trend while blue denotes it was a climate reversal. Plot of the Younger Dryas (YD) fraction of the G-IG change relative to latitude (b). (For interpretation of the references to colour in this figure legend, the reader is referred to the web version of this article.)

(Huybers and Denton, 2008). Our compilation of LGM records points to the difficulty in determining leads and lags between the hemispheres in the timing of LGM termination. Given the large spread in the timing of the LGM in both hemispheres, caution should be taken when selecting only one or several records for the basis of arguments on the forcing and phasing of orbital scale climate change.

The timing of the Northern Hemisphere Altithermal at 8.0 ± 3.2 ka (Fig. 4) is consistent with forcing from boreal summer insolation in combination with greenhouse gases. The ~ 4 kyr lag behind peak insolation may, in part, reflect the effects of the waning Northern Hemisphere ice sheets, which did not completely disappear until ~ 6.5 ka (Antevs, 1953; Kaufman et al., 2004; Kaplan and Wolfe,

2006; Carlson et al., 2007b, 2008a). While the Southern Hemisphere also has a modest peak in the early Holocene (Fig. 4b), there is a more even distribution of Altithermal ages throughout the Holocene than the Northern Hemisphere, suggesting that the concept of a peak interglacial climate state may not be as meaningful in the Southern Hemisphere.

The different magnitudes of glacial-interglacial temperature changes between the hemispheres (Fig. 5) are consistent with multiple forcing/feedback mechanisms of glacial cooling for each hemisphere. In the Northern Hemisphere, the expansion of large ice sheets and North Atlantic sea ice, lower greenhouse gases, and changes in vegetation and aerosols likely combined to produce the LGM climate (Manabe and Broccoli, 1985; Broccoli,

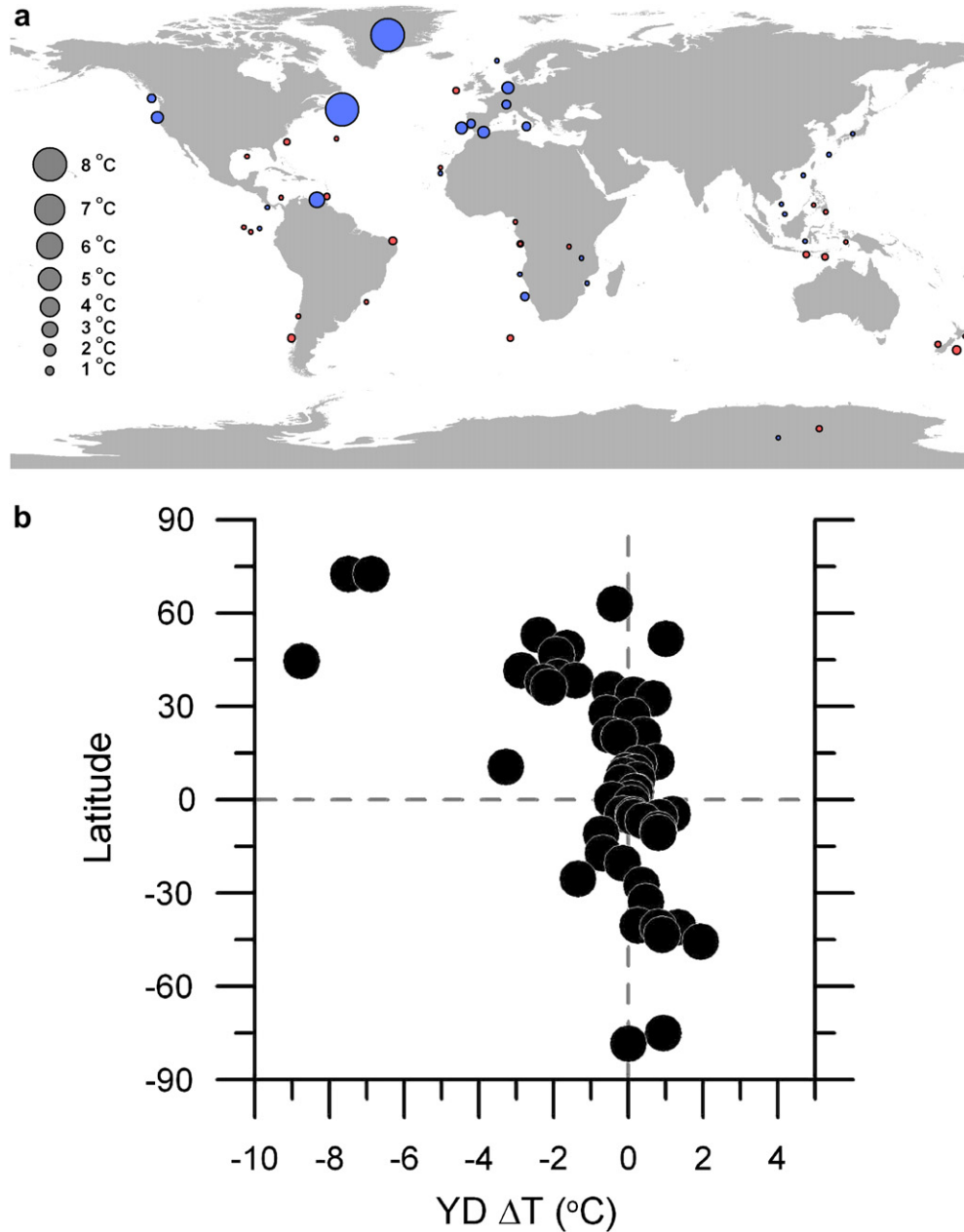


Fig. 12. Magnitude of the Younger Dryas temperature change. Map of the Younger Dryas temperature anomaly (a). Circle denotes the size of the temperature change. Blue is cooling, red warming. Plot of the Younger Dryas (YD) temperature anomaly relative to latitude (b). (For interpretation of the references to colour in this figure legend, the reader is referred to the web version of this article.)

2000; Otto-Bliesner et al., 2006; Schneider von Deimling et al., 2006; Braconnot et al., 2007). In the Southern Hemisphere, the continental shelf edge limited the expansion of the only major ice sheet (Antarctic) suggesting that Southern Ocean sea ice expansion, lowered greenhouse gases, and increased aerosols were the major drivers of Southern Hemisphere LGM climate (Imbrie et al., 1993; Gildor and Tziperman, 2001; Otto-Bliesner et al., 2006; Braconnot et al., 2007; Lambert et al., 2008). Thus, the large ice sheet forcing may account for much of the greater cooling and steeper meridional temperature gradient in the Northern Hemisphere relative to the Southern Hemisphere (Fig. 5).

The EOF results identify major drivers of climate change over the deglaciation. The agreement between 19 and 11 ka PC1 and atmospheric CO_2 implicates the carbon cycle as an important

feedback of global deglacial climate change (Figs. 6b and 7) (Chamberlin, 1897; Mix et al., 1986a; Visser et al., 2003; Lea et al., 2006; Otto-Bliesner et al., 2006). The correlation between 19 and 11 ka PC2 and AMOC strength supports arguments that variations in AMOC are another important deglacial climate forcing with a bipolar seesaw climate response (Broecker, 1998; Blunier and Brook, 2001; Clark et al., 2002; Liu et al., 2009) (Figs. 6c and 8). Indeed, the climate effects of the initial decrease in AMOC strength at ~ 19 ka to a minimum during the Oldest Dryas are well-represented in PC2 (Fig. 8). The attendant bipolar seesaw climate response (Northern Hemisphere cooling/drying, Southern Hemisphere warming/wetting) to this AMOC reduction may help explain the often noted "lead" in Southern Hemisphere climate (e.g., Shackleton, 2000; Koutavas et al., 2002; Visser et al., 2003; Lea et al., 2006; Stott et al., 2007) over Northern Hemisphere climate

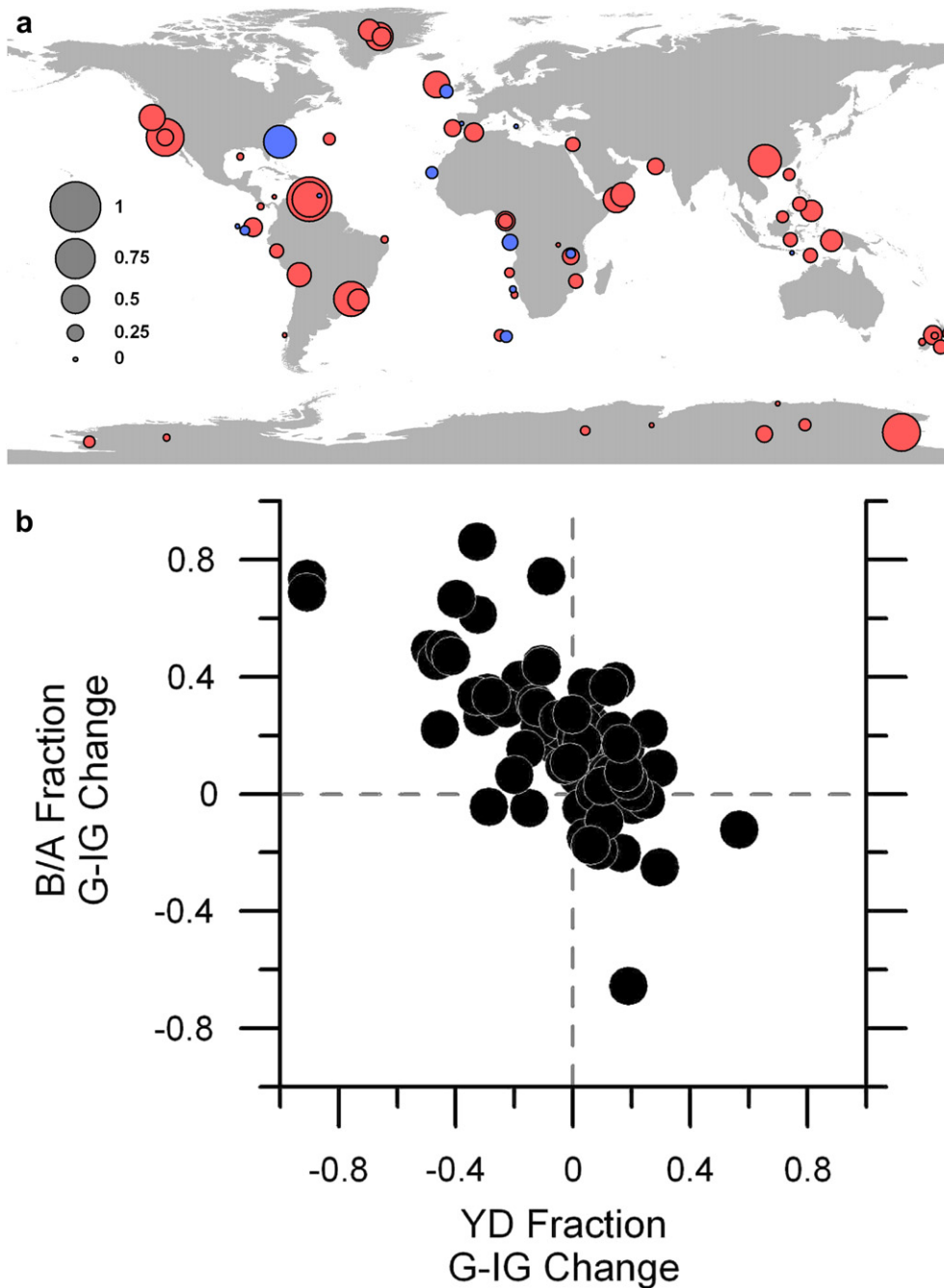


Fig. 13. Magnitude of Bølling/Allerød climate change. Map of the Bølling/Allerød fraction of the glacial–interglacial (G–IG) change (a). Red denotes Bølling/Allerød was continuation of deglacial trend while blue denotes it was a climate reversal. Magnitude of the Younger Dryas (YD) anomaly versus the Bølling/Allerød (B/A) anomaly (b). (For interpretation of the references to colour in this figure legend, the reader is referred to the web version of this article.)

and ice sheets (Alley et al., 2002; Clark et al., 2004, 2009; Carlson et al., 2008b).

AMOC variability was expressed as relatively coherent northern and southern climate modes in the higher latitudes of each hemisphere, whereas the climate response was spatially more variable in the low latitudes (see Sections 3.3 and 4.1). This difference may reflect the larger number of climate variables recorded by proxies as well as the variety of transmission mechanisms operating in different subtropical and tropical regions. For example, a reduction in AMOC during the Younger Dryas would cause a southward shift in the ITCZ, changing latitudinal precipitation and wind patterns as well as upwelling regimes (Mix et al., 1986b; Haug et al., 2001;

Chiang et al., 2003; Lea et al., 2003; Chiang and Bitz, 2005; Zhang and Delworth, 2005; Benway et al., 2006). Reduced northward heat transport associated with weakened AMOC may store heat in the subtropics and tropics of the western Atlantic (Crowley, 1992; Rühlemann et al., 1999; Schmidt et al., 2004; Grimm et al., 2006; Weldeab et al., 2006; Carlson et al., 2008c), causing warming during an overall North Atlantic cooling event. Another polar connection to the tropics is via the oceanic tunnel of thermocline subduction and the atmospheric bridge of the Hadley Circulation (Liu and Yang, 2003). Warming of Southern Ocean thermocline water (at the end of the Antarctic Cold Reversal) from a reduction in AMOC strength (Schmittner et al., 2003) may crop out in the

tropical surface ocean within decades causing tropical warming during the Younger Dryas. Therefore, the bipolar seesaw behavior at the high latitudes of the two hemispheres (Bølling/Allerød warming–Antarctic Cold Reversal followed by Younger Dryas cooling–termination of Antarctic Cold Reversal) (Broecker, 1998; Blunier and Brook, 2001; Clark et al., 2002; Weaver et al., 2003) may have affected different tropical-subtropical regions possibly at different times.

Bipolar seesaw temperature responses during the Younger Dryas are likewise best expressed in the mid to high latitudes of each hemisphere, but less clear in the low latitudes. North Hemisphere cooling of 2–8 °C is evident above ~35°N whereas Southern Hemisphere warming of 1–2 °C is apparent below ~45°S (Fig. 12). The tropical and subtropical temperature changes, in contrast, are between –1 and +1 °C (with the exception of Cariaco Basin, –3.3 °C; Lea et al., 2003), or ~0 °C when considering the error in calculating temperature from proxies (e.g., Mg/Ca, U^k₃₇; Lea, 2003). We suggest that the seesaw model does not adequately represent tropical temperature variability, which instead seems to be predominantly controlled by greenhouse gases. Lower latitude precipitation does appear to exhibit a seesaw pattern, however.

All of the patterns discussed above suggest a northern high latitude origin for the Younger Dryas cold event, because (1) the largest negative climate anomalies occur in the extratropical Northern Hemisphere focused around the North Atlantic, (2) there is a variable expression of the Younger Dryas in both sign and magnitude in the tropics and subtropics, and (3) modest positive climate anomalies occur in the extratropical Southern Hemisphere (Figs. 11 and 12). This is consistent with the Younger Dryas being a redistribution of heat, as would accompany a reduction in AMOC strength (Fig. 8), rather than a global-scale cooling event, which requires a change in the planetary energy balance. Younger Dryas cooling in the north does appear to slightly outweigh warming in the south, however, with a global mean cooling of ~0.6 °C (Fig. 12b). As greenhouse gases, insolation, and global ice volume were nearly unchanged from the Allerød to the Younger Dryas (Fig. 7), a net global cooling could most plausibly be explained by increased Northern Hemisphere albedo due to greater snow and sea ice cover and aerosol loading (Alley, 2000; Denton et al., 2005). This small global mean temperature decrease during the Younger Dryas relative to the global cooling of ~4.9 °C at the LGM would suggest that the Younger Dryas was hardly a return to ice age climate. It is instead on par with the global cooling of ~0.8 °C during the Little Ice Age relative to the present (Mann et al., 2008).

Several other differences stand out between the Younger Dryas and the LGM. Meridional temperature gradients were generally smaller for the Younger Dryas. One hemisphere warmed while the other cooled during the Younger Dryas whereas both were colder during the LGM. Tropical temperatures were largely unaffected by the Younger Dryas with an average temperature change of 0.0 ± 0.8 °C ($n = 31$), but the tropics cooled by 2.5 ± 0.9 °C ($n = 28$) during the LGM. Moreover, temperature anomalies during the LGM were generally several times larger than those during the Younger Dryas (Figs. 5 and 11). One similarity, however, is that greater climate change occurred in the Northern Hemisphere than in the Southern Hemisphere and the meridional temperature gradient steepened considerably in the northern extratropics, suggesting the northern higher latitudes may be more sensitive to climate change.

Arguments for Southern Hemisphere cooling, and thus global cooling, during the Younger Dryas are predominately based on valley glacier records constrained by limiting radiocarbon dates (Broecker, 1994, 2003; Denton and Hendy, 1994; Lowell et al., 1995; Ariztegui et al., 1997; Denton et al., 1999b). The most often cited record is the Waiho Loop Moraine of New Zealand (Denton and Hendy, 1994). The majority of Waiho radiocarbon dates, however, precede the

onset of the Younger Dryas (Broecker, 2003), a result recently confirmed by Turney et al. (2007). Moreover, this moraine may not represent a climatic event, but rather an anomalous landslide-triggered glacier advance through the insulating effect of the debris (Tovar et al., 2008). Much work has recently applied cosmogenic dating to late-glacial Southern Hemisphere moraines to address the extent of the Younger Dryas (Strelin and Malagnino, 2000; Douglass et al., 2005, 2006; McCulloch et al., 2005; Sugden, 2005; Sugden et al., 2005; Barrows et al., 2007b; Kilian et al., 2007; Ackert et al., 2008; Kaplan et al., 2008; Moreno et al., 2009). Given current debates on the limitations in dating glacial events (Applegate et al., 2008; Barrows et al., 2008; Lowell and Kelly, 2008; Putnam et al., 2010), however, these glacial records do not at present provide strong evidence for or against Southern Hemisphere cooling during the Younger Dryas. We suggest that the modes of deglacial climate variability identified in our analyses of high-resolution, well-dated climate records predict Southern Hemisphere moraines of Younger Dryas age are, in general, unlikely to be found.

The main mechanism proposed for atmospheric, and not AMOC, forcing of the Younger Dryas calls on El Niño–Southern Oscillation (ENSO)-like processes originating in the tropics (Cane and Clement, 1999; Clement and Cane, 1999; Clement et al., 2001; Broecker, 2003; Clement and Peterson, 2008). Such a scenario would likely result in three observable patterns. Presumably, ENSO-like forcing would produce (1) interhemispheric symmetry in the response of the climate system (Hoerling and Kumar, 2000; Seager et al., 2005), (2) a marked change in the global energy balance via changes in planetary albedo and greenhouse trapping (Cane and Clement, 1999; Thompson et al., 2008), and (3) the largest climate signals in the tropics (Ropelewski and Halpert, 1987; Mantua and Hare, 2002) as occurs with modern ENSO variability. The analyses presented above contradict these predictions, and rather demonstrate the existence of two different hemispheric modes of climate variability that are most pronounced at higher latitudes and interact in a complex manner in the tropics. They also suggest a relatively diminutive perturbation to the planetary energy budget during the Younger Dryas, which in any case was driven largely by the northern high latitudes and not the tropics.

6. Conclusions

There are five main conclusions drawn from these analyses of deglacial climate records.

- (1) The timing of the LGM and Altithermal varied considerably around the globe but were statistically synchronous between the hemispheres. The LGM and Altithermal occurred at 22.1 ± 4.3 ka and 8.0 ± 3.2 ka in the Northern Hemisphere and 22.3 ± 3.6 ka and 7.4 ± 3.7 ka in the Southern Hemisphere, respectively. Global mean cooling during the LGM was likely at least ~4.9 °C relative to the Altithermal.
- (2) The first mode of deglacial climate variability is common to most climate records and is likely related to rising CO₂, implicating it as a major deglacial forcing/feedback.
- (3) The second mode of deglacial climate variability shows a bipolar seesaw pattern between the hemispheres most likely driven by fluctuations in AMOC strength. This bipolar climate pattern may partly explain the apparent “lead” of Southern Hemisphere climate over Northern Hemisphere climate and ice sheets.
- (4) The Bølling/Allerød–Younger Dryas climate oscillations were an expression of this bipolar seesaw with the Antarctic Cold Reversal representing the opposite sign response of the Southern Hemisphere. However, these climate events are most clear at mid to high latitudes with a complex climate response in the tropics and subtropics of both hemispheres.

(5) While the Younger Dryas may have been a near-global scale climate change, in the sense that climatic anomalies occurred in many regions during this time, it was not a major global cooling event (approximately -0.6°C change), with many records showing warming or a shift toward interglacial conditions through the Younger Dryas. This is particularly evident in the low latitudes of the Northern Hemisphere and in many areas of the Southern Hemisphere. Globally, the Younger Dryas was by no means a return to ice age climate.

Acknowledgements

The authors would like to thank P. Clark, J. Kutzbach, S. Marcott, A. Mix, N. Pisias, and J. Shaman for helpful discussions, and T. Bauska, P. Clark, S. Marcott for reading an earlier version of this manuscript. Four anonymous reviewers improved the clarity of the original manuscript. J. Shakun is funded by the National Science Foundation Paleoclimate Program. A. Carlson is funded by the National Science Foundation Paleoclimate Program and University of Wisconsin-Madison start-up funds. Datasets were graciously provided by J. Andrews, S. Burns, T. Barrows, P. Clark, O.M. Heiri, J. Hellstrom, I. Hendy, F.S. Hu, L. Labeyrie, V. Peck, C. Pelejero, J. Sachs, E. Schefub, J. Tierney, and P. Williams. The authors would also like to acknowledge the extensive databases provided by NOAA NGDC and PANGAEA.

Appendix A. Supplementary information

Supplementary data associated with this article can be found, in the online version, at doi:10.1016/j.quascirev.2010.03.016.

References

- Ackert Jr., R.P., Becker, R.A., Singer, B.S., Kurz, M.D., Caffee, M.W., Mickelson, D.M., 2008. Patagonian glacier response during the late glacial-Holocene transition. *Science* 321, 392–395.
- Ahn, J., Wahlen, M., Deck, B.L., Brook, E.J., Mayewski, P.A., Taylor, K.C., White, J.W.C., 2004. A record of atmospheric CO_2 during the last 40,000 years from the Siple Dome, Antarctica ice core. *Journal of Geophysical Research* 109. doi:10.1029/2003JD004415.
- Ahn, J., Brook, E.J., 2008. Atmospheric CO_2 and climate on millennial time scales during the last glacial period. *Science* 322, 83–85.
- Alley, R.B., 2000. The Younger Dryas cold interval as viewed from central Greenland. *Quaternary Science Reviews* 19, 213–226.
- Alley, R.B., Brook, E.J., Anandkrishnan, S., 2002. A northern lead in the orbital band: north-south phasing of Ice-Age events. *Quaternary Science Reviews* 21, 431–441.
- Alley, R.B., Clark, P.U., 1999. The deglaciation of the northern hemisphere: a global perspective. *Annual Reviews of Earth and Planetary Sciences* 27, 149–182.
- Antevs, E., 1953. Geochronology of the deglacial and neothermal ages. *The Journal of Geology* 61, 195–230.
- Applegate, P.J., Lowell, T.V., Alley, R.B., 2008. Comment on “Absence of cooling in New Zealand and the adjacent Ocean during the Younger Dryas chronozone”. *Science* 320, 746.
- Ariztegui, D., Bianchi, M.M., Masafiero, J., Lafargue, E., Niessen, F., 1997. Interhemispheric synchrony of Late-glacial climatic instability as recorded in proglacial Lake Mascardina, Argentina. *Journal of Quaternary Science* 12, 333–338.
- Barker, S., Diz, P., Vautravers, M.J., Pike, J., Knorr, G., Hall, I.R., Broecker, W.S., 2009. Interhemispheric Atlantic seesaw response during the last deglaciation. *Nature* 457, 1097–1102.
- Barrows, T.T., Juggins, S., De Deckker, P., Calvo, E., Pelejero, C., 2007a. Long-term sea surface temperature and climate change in the Australian–New Zealand region. *Paleoceanography* 22. doi:10.1029/2006PA001328.
- Barrows, T.T., Lehman, S.J., Fifield, L.K., De Deckker, P., 2007b. Absence of cooling in New Zealand and the adjacent Ocean during the Younger Dryas chronozone. *Science* 318, 86–89.
- Barrows, T.T., Lehman, S.J., Fifield, L.K., De Deckker, P., 2008. Response to comment on “Absence of cooling in New Zealand and the adjacent Ocean during the Younger Dryas chronozone”. *Science* 320, 746.
- Benway, H.M., Mix, A.C., Haley, B.A., Klinkhammer, G.P., 2006. Eastern Pacific warm pool paleosalinity and climate variability: 0–30 kyr. *Paleoceanography* 21. doi:10.1029/2005PA001208.
- Berger, A., Loutre, M.-F., 1991. Insolation values for the climate of the last 10 million years. *Quaternary Science Reviews* 10, 297–317.
- Blunier, T., Brook, E.J., 2001. Timing of millennial-scale climate change in Antarctica and Greenland during the last glacial period. *Science* 291, 109–112.
- Boyle, E.A., Keigwin, L., 1987. North Atlantic thermohaline circulation during the past 20,000 years linked to high-latitude surface temperature. *Nature* 330, 35–40.
- Braconnot, P., Otto-Bliesner, B., Harrison, S., Joussaume, S., Peterchmitt, J.-Y., Abe-Ouchi, A., Crucifix, M., Driesschaert, E., Fichefet, T., Hewitt, C.D., Kageyama, M., Kitoh, A., Loutre, M.-F., Marti, O., Merkel, U., Ramstein, G., Valdes, P., Weber, L., Yu, Y., Zhao, Y., 2007. Results of PMIP2 coupled simulations of the mid-Holocene and Last Glacial Maximum – part 2: feedbacks with emphasis on the location of the ITCZ and mid- and high latitudes heat budget. *Climate of the Past* 3, 279–296.
- Broccoli, A.J., 2000. Tropical cooling at the Last Glacial Maximum: an atmosphere-mixed layer ocean model simulation. *Journal of Climate* 13, 951–976.
- Broecker, W.S., 1994. Massive iceberg discharges as triggers for global climate change. *Nature* 372, 421–424.
- Broecker, W.S., 1998. Paleocirculation during the last deglaciation: a bipolar seesaw? *Paleoceanography* 13, 119–121.
- Broecker, W.S., 2003. Does the trigger for abrupt climate change reside in the ocean or in the atmosphere? *Science* 300, 1519–1522.
- Cane, M., Clement, A.C., 1999. A role for the tropical Pacific coupled ocean-atmosphere system on Milankovitch and millennial timescales. Part II: global impacts. In: Clark, P.U., Webb, R.S., Keigwin, L.D. (Eds.), *Mechanisms of Global Climate Change at Millennial Time Scales*. American Geophysical Union, Washington, D.C., pp. 373–383.
- Carlson, A.E., Clark, P.U., Haley, B.A., Klinkhammer, G.P., Simmons, K.R., Brook, E., Meissner, K.J., 2007a. Geochemical proxies of North American freshwater routing during the Younger Dryas. *Proceedings of the National Academy of Sciences* 104, 6556–6561.
- Carlson, A.E., Clark, P.U., Raisbeck, G.M., Brook, E.J., 2007b. Rapid Holocene deglaciation of the Labrador sector of the Laurentide Ice Sheet. *Journal of Climate* 20, 5126–5133.
- Carlson, A.E., LeGrande, A.N., Oppo, D.W., Came, R.E., Schmidt, G.A., Anslow, F.S., Licciardi, J.M., Obbink, E.A., 2008a. Rapid early Holocene deglaciation of the Laurentide ice sheet. *Nature Geoscience* 1, 620–624.
- Carlson, A.E., Stoner, J.S., Donnelly, J.P., Hillaire-Marcel, C., 2008b. Response of the southern Greenland Ice Sheet during the last two deglaciations. *Geology* 36, 359–362.
- Carlson, A.E., Oppo, D., Came, R.E., LeGrande, A.N., Keigwin, L., Curry, W.B., 2008c. Subtropical salinity variability and Atlantic meridional circulation during deglaciation. *Geology* 12, 991–994.
- Chamberlin, T.C., 1897. A group of hypotheses bearing on climatic changes. *Journal of Geology* 5, 653–683.
- Chiang, J.C.H., Biasutti, M., Battisti, D.S., 2003. Sensitivity of the Atlantic ITCZ to Last Glacial Maximum boundary conditions. *Paleoceanography* 18. doi:10.1029/2003PA000916.
- Chiang, J.C.H., Bitz, C.M., 2005. The influence of high latitude ice on the position of the marine intertropical convergence zone. *Climate Dynamics*. doi:10.1007/s00382-005-0040-5.
- Clark, P.U., Mix, A.C., 2002. Ice sheets and sea level of the Last Glacial Maximum. *Quaternary Science Reviews* 21, 1–7.
- Clark, P.U., Pisias, N.G., Stocker, T.F., Weaver, A.J., 2002. The role of the thermohaline circulation in abrupt climate change. *Nature* 415, 863–869.
- Clark, P.U., McCabe, A.M., Mix, A.C., Weaver, A.J., 2004. Rapid rise of sea level 19,000 years ago and its global implications. *Science* 304, 1141–1144.
- Clark, P.U., Hostetler, S., Pisias, N., Schmittner, A., Meissner, K.J., 2007. Mechanisms for a ~7-kyr climate and sea-level oscillation during marine isotope stage 3. In: Schmittner, A., Chiang, J.C.H., Hemming, S. (Eds.), *Ocean Circulation: Mechanisms and Impacts*. American Geophysical Union, Washington, D.C., pp. 315–334.
- Clark, P.U., Dyke, A.S., Shakun, J.D., Carlson, A.E., Clark, J., Wohlfarth, B., Hostetler, S.W., McCabe, A.M., 2009. The Last Glacial Maximum. *Science* 325, 710–714.
- Clement, A.C., Cane, M.A., 1999. A role for the tropical Pacific coupled ocean-atmosphere system on Milankovitch and millennial timescales. Part II: A modeling study of tropical Pacific variability. In: Clark, P.U., Webb, R.S., Keigwin, L.D. (Eds.), *Mechanisms of Global Climate Change at Millennial Time Scales*. American Geophysical Union, Washington, D.C., pp. 363–371.
- Clement, A.C., Cane, M.A., Seager, R., 2001. An orbitally driven tropical source for abrupt climate change. *Journal of Climate* 14, 2369–2375.
- Clement, A.C., Peterson, L.C., 2008. Mechanisms of abrupt climate change of the last glacial period. *Reviews of Geophysics* 46. doi:10.1029/2006RG000204.
- CLIMAP Project Members, 1976. The surface of the ice-age earth. *Science* 191, 1131–1137.
- Crowley, T.J., 1992. North Atlantic deep water cools the Southern Hemisphere. *Paleoceanography* 7, 489–497.
- Cuffey, K., Clow, G.D., 1997. Temperature, accumulation, and ice sheet elevation in central Greenland through the last deglacial transition. *Journal of Geophysical Research* 102, 26383–26396.
- Denton, G.H., Hendy, C.H., 1994. Younger Dryas age advance of Franz Josef glacier in the Southern Alps of New Zealand. *Science* 264, 1434–1437.
- Denton, G.H., Heusser, C.J., Lowell, T.V., Moreno, P.J., Andersen, B.G., Huesser, L.E., Schlüchter, C., Marchant, D.R., 1999a. Interhemispheric linkage of paleoclimate during the last glacial period. *Geografiska Annaler* 81A, 107–153.
- Denton, G.H., Andersen, B.G., Heusser, L.E., Moreno, P.J., Marchant, D.R., Lowell, T.V., Heusser, C.J., Schlüchter, C., 1999b. Geomorphology, stratigraphy, and radiocarbon chronology of Llanquihue drift in the area of the southern Lake District, Seno Reloncavi, and Isla Grande de Chiloe, Chile. *Geographiska Annaler Series A: Physical Geography* 81, 167–229.

- Denton, G.H., Alley, R.B., Comer, G.C., Broecker, W.S., 2005. The role of seasonality in abrupt climate change. *Quaternary Science Reviews* 24, 1159–1182.
- Douglas, D.C., Singer, B.S., Kaplan, M.R., Ackert, R.P., Mickelson, D.M., Caffee, M.W., 2005. Evidence of early Holocene glacial advances in southern South America from cosmogenic surface-exposure dating. *Geology* 33, 237–240.
- Douglas, D.C., Singer, B.S., Kaplan, M.R., Mickelson, D.M., Caffee, M.W., 2006. Cosmogenic nuclide surface exposure dating of boulders on last-glacial and late-glacial moraines, Lago Buenos Aires, Argentina: interpretive strategies and paleoclimate implications. *Quaternary Geochronology* 1, 43–58.
- Gildor, H., Tziperman, E., 2001. Physical mechanisms behind biogeochemical glacial-interglacial CO₂ variations. *Geophysical Research Letters* 28, 2421–2424.
- Grimm, E.C., Watts, W.A., Jacobson, J.G.L., Hansen, B.C.S., Almquist, H.R., Dieffenbacher-Krall, A.C., 2006. Evidence for warm wet Heinrich events in Florida. *Quaternary Science Reviews* 25, 2197–2211.
- Haug, G.H., Hughen, K.A., Sigman, D.M., Peterson, L.C., Rohl, U., 2001. Southward migration of the Intertropical Convergence Zone through the Holocene. *Science* 293, 1304–1308.
- Hoerling, T.C., Kumar, A., 2000. Understanding and predicting extratropical teleconnections related to ENSO. In: Diaz, H., Markgraf, V. (Eds.), *El Niño and the Southern Oscillation: Multi-scale Variability, and Global and Regional Impacts*. Cambridge University Press, pp. 57–88.
- Huësser, C.J., Rabassa, J., 1987. Cold climatic episode of Younger Dryas age in Tierra del Fuego. *Nature* 328, 609–611.
- Huybers, P., Denton, G., 2008. Antarctic temperature at orbital timescales controlled by local summer duration. *Nature Geoscience* 1, 787–792.
- Imbrie, J., Berger, A., Boyle, E.A., Clemens, S.C., Duffy, A., Howard, W.R., Kukla, G., Kutzbach, J., Martinson, D.G., McIntyre, A., Mix, A.C., Molino, B., Morley, J.J., Peterson, L.C., Pisias, N.G., Prell, W.L., Raymo, M.E., Shackleton, N.J., Toggweiler, J. R., 1993. On the structure and origin of major glacial cycles. 2. The 100,000-year cycle. *Paleoceanography* 8, 699–735.
- Ivy-Ochs, S., Schlüchter, C., Kubik, P.W., Denton, G.H., 1999. Moraine exposure dates imply synchronous Younger Dryas glacier advances in the European Alps and in the Southern Alps of New Zealand. *Geografiska Annaler* 81, 313–323.
- Jouzel, J., Vaikmae, R., Petit, J.R., Martin, M., Duclos, Y., Stevenard, M., Lorius, C., Toots, M., Melieres, M.A., Burckle, L.H., Barkov, N.I., Kotlyakov, V.M., 1995. The two-step shape and timing of the last deglaciation in Antarctica. *Climate Dynamics* 11, 151–161.
- Kaplan, M.R., Wolfe, A.P., 2006. Spatial and temporal variability of Holocene temperature in the North Atlantic region. *Quaternary Research* 65, 223–231.
- Kaplan, M.R., Fogwill, C.J., Sugden, D.E., Hulton, N.R.J., Kubik, P.W., Freeman, S.P.H.T., 2008. Southern Patagonian glacial chronology for the Last Glacial period and implications for Southern Ocean climate. *Quaternary Science Reviews* 27, 284–294.
- Kaufman, D.S., Ager, T.A., Anderson, N.J., Anderson, P.M., Andrews, J.T., Bartlein, P.J., Brubaker, L.B., Coats, L.L., Cwynar, L.C., Duvall, M.L., Dyke, A.S., Edwards, M.E., Eisner, W.R., Gajewski, K., Geirsdóttir, A., Hu, F.S., Jennings, A.E., Kaplan, M.R., Kerwin, M.W., Lozhkin, A.V., MacDonald, G.M., Miller, G.H., Mock, C.J., Oswald, W.W., Otto-Bliesner, B.L., Porinchu, D.F., Rühland, K., Smol, J.P., Steig, E. J., Wolfe, B.B., 2004. Holocene thermal maximum in the western Arctic (0–180°W). *Quaternary Science Reviews* 23, 529–560.
- Kawamura, K., Parrenin, F., Lisiecki, L., Uemura, R., Vimeux, F., Severinghaus, J.P., Hutterli, M.A., Nakazawa, T., Aoki, S., Jouzel, J., Raymo, M.E., Matsumoto, K., Nakata, H., Motoyama, H., Fujita, S., Goto-Azuma, K., Fujii, Y., Watanabe, O., 2007. Northern Hemisphere forcing of climatic cycles in Antarctica over the past 360,000 years. *Nature* 448, 912–916.
- Kilian, R., Schneider, C., Koch, J., Fesq-Martin, M., Biester, H., Casassa, G., Arealo, M., Wendt, G., Baeza, O., Behrmann, J., 2007. Palaeoecological constraints on late Glacial and Holocene ice retreat in the Southern Andes (53°S). *Global and Planetary Change* 59, 49–66.
- Koutavas, A., Lynch-Stieglitz, J., Marchitto Jr., T.M., Sachs, J.M., 2002. El Niño-like pattern in Ice Age tropical Pacific sea surface temperature. *Science* 297, 226–230.
- Lambert, F., Delmonte, B., Petit, J.R., Bigler, M., Kaufman, P.R., Hutterli, M.A., Stocker, T. F., Ruth, U., Steffensen, J.P., Maggi, V., 2008. Dust-climate couplings over the past 800,000 years from the EPICA Dome C ice core. *Nature* 452, 616–619.
- Lea, D.W., 2003. Elemental and isotopic proxies of marine temperatures. In: Elderfield, H. (Ed.), *The Oceans and Geochemistry*. Elsevier-Perгамon, Oxford, pp. 365–390.
- Lea, D.W., Pak, D.K., Peterson, L.C., Hughen, K.A., 2003. Synchronicity of tropical and high-latitude Atlantic temperatures over the last glacial termination. *Science* 301, 1361–1364.
- Lea, D.W., Pak, D.K., Belanger, C.L., Spero, H.J., Hall, M.A., Shackleton, N.J., 2006. Paleoclimate history of Galápagos surface waters over the last 135,000 yr. *Quaternary Science Reviews* 25, 1152–1167.
- Liu, Z., Yang, H., 2003. Extratropical control on tropical climate: atmospheric bridge and oceanic tunnel. *Geophysical Research Letters* 30. doi:10.1029/2002GL016492.
- Liu, Z., Otto-Bliesner, B., He, F., Brady, E., Thomas, R., Clark, P.U., Carlson, A.E., Lynch-Stieglitz, J., Curry, W., Brook, E., Erickson, D., Jacob, R., Kutzbach, J., Chen, J., 2009. Transient climate simulation of last deglaciation with a new mechanism for Bølling-Allerød warming. *Science* 325, 310–314.
- Lowell, T.V., Heusser, C.J., Andersen, B.G., Moreno, P.I., Hauser, A., Heusser, L.E., Schluchter, C., Marchant, D.R., Denton, G.H., 1995. Interhemispheric correlation of Late Pleistocene glacial events. *Science* 269, 1541–1549.
- Lowell, T.V., Kelly, M.A., 2008. Was the Younger Dryas global? *Science* 321, 348–349.
- Manabe, S., Broccoli, A.J., 1985. The influence of continental ice sheets on the climate of an ice age. *Journal of Geophysical Research* 90, 2167–2190.
- Mann, M.E., Zhangk, Z., Hughes, M.K., Bradley, R.S., Miller, S.K., Rutherford, S., Ni, F., 2008. Proxy-based reconstructions of hemispheric and global surface temperature variations over the past two millennia. *Proceedings of the National Academy of Sciences* 105, 13252–13257.
- Mantua, N.J., Hare, S.R., 2002. The Pacific decadal oscillation. *Journal of Oceanography* 58, 35–44.
- McCulloch, R.D., Fogwill, C.J., Sugden, D.E., Bentley, M.J., Kubik, P.W., 2005. Chronology of the last glaciation in central Strait of Magellan and Bahía Inútil, southernmost South America. *Geografiska Annaler* 87, 289–312.
- McManus, J.F., Francois, R., Gherardi, J.M., Keigwin, L.D., Brown-Leger, S., 2004. Collapse and rapid resumption of Atlantic meridional circulation linked to deglacial climate changes. *Nature* 428, 834–837.
- Mix, A.C., 2006. Running hot and cold in the eastern equatorial Pacific. *Quaternary Science Reviews* 25, 1147–1149.
- Mix, A.C., Ruddiman, W.F., McIntyre, A., 1986a. Late Quaternary paleoceanography of the tropical Atlantic, 1: spatial variability of annual mean sea-surface temperatures 0–20,000 years B.P. *Paleoceanography* 1, 43–66.
- Mix, A.C., Ruddiman, W.F., McIntyre, A., 1986b. Late Quaternary paleoceanography of the tropical Atlantic, 2: the seasonal cycle of sea surface temperatures, 0–20,000 years B.P. *Paleoceanography* 1, 339–353.
- Mix, A.C., Bard, E., Schneider, R., 2001. Environmental processes of the ice age: land, ocean, glaciers (EPILOG). *Quaternary Science Reviews* 20, 627–657.
- Monnin, E., Indermühle, A., Dällenbach, A., Flückiger, J., Stauffer, B., Stocker, T.F., Raynaud, D., Barnola, J.-M., 2001. Atmospheric CO₂ concentrations over the last glacial termination. *Science* 291, 112–114.
- Moreno, P.I., Jacobson, G.L.J., Lowell, T.V., Denton, G.H., 2001. Interhemispheric climate links revealed by a late-glacial cooling episode in southern Chile. *Nature* 409, 804–808.
- Moreno, P.I., Kaplan, M.R., François, J.P., Villa-Martínez, R., Moy, C.M., Stern, C.R., Kubik, P.W., 2009. Renewed glacial activity during the Antarctic cold reversal and persistence of cold conditions until 11.5 ka in southwestern Patagonia. *Geology* 37, 375–378.
- Otto-Bliesner, B.L., Brady, E.C., Clauzet, G., Tomas, R., Levis, S., Kothavala, Z., 2006. Last Glacial Maximum and Holocene climate in CCSM3. *Journal of Climate* 19, 2526–2544.
- Petee, D., 1995. Global Younger Dryas? *Quaternary International* 28, 93–104.
- Pinot, S., Ramstein, G., Harrison, S.P., Prentice, I.C., Guiot, J., Stute, M., Joussaume, S., 1999. Tropical paleoclimates at the Last Glacial Maximum: comparison of Paleoclimate Modeling Intercomparison Project (PMIP) simulations and paleodata. *Climate Dynamics* 15, 857–874.
- Putnam, A.E., Schaefer, J.M., Barrell, D.J.A., Vandergoes, M., Denton, G.H., Kaplan, M. R., Finkel, R.C., Schwartz, R., Goehring, B.M., Kelley, S.E., 2010. In situ cosmogenic ¹⁰Be production-rate calibration from the Southern Alps, New Zealand. *Quaternary Geochronology*. doi:10.1016/j.quageo.2009.12.001.
- Rasmussen, S.O., Andersen, K.K., Svensson, A.M., Steffensen, J.P., Vinther, B.M., Clausen, H.B., Siggaard-Andersen, M.-L., Johnsen, S.J., Larsen, L.B., Dahl-Jensen, D., Bigler, M., Rothlisberger, R., Fischer, H., Goto-Azuma, K., Hansson, M., Ruth, U., 2006. A new Greenland ice core chronology of the last glacial termination. *Journal of Geophysical Research* 111. doi:10.1029/2005JD006079.
- Robinson, L.F., Adkins, J.F., Keigwin, L.D., Southon, J., Fernandez, D.P., Wang, S.L., Scheirer, D.S., 2005. Radiocarbon variability in the western North Atlantic during the last deglaciation. *Science* 310, 1469–1473.
- Ropelewski, C.F., Halpert, M.S., 1987. Global and regional scale precipitation patterns associated with the El Niño/Southern Oscillation (ENSO). *Monthly Weather Review* 115, 1606–1626.
- Rühlemann, C., Mulitza, S., Müller, P.J., Wefer, G., Zahn, R., 1999. Warming of the tropical Atlantic Ocean and slowdown of thermohaline circulation during the last deglaciation. *Nature* 402, 511–514.
- Schmidt, M.W., Spero, H.J., Lea, D.W., 2004. Links between salinity variation in the Caribbean and North Atlantic thermohaline circulation. *Nature* 428, 160–163.
- Schmittner, A., Saenko, O., Weaver, A.J., 2003. Coupling of the hemispheres in observations and simulations of glacial climate change. *Quaternary Science Reviews* 22, 659–672.
- Schneider von Deimling, T., Ganopolski, A., Held, H., Rahmstorf, S., 2006. How cold was the Last Glacial Maximum? *Geophysical Research Letters* 33. doi:10.1029/2006GL026484.
- Seager, R., Harnik, N., Robinson, W.A., Kushnir, Y., Ting, M.F., Huang, H.P., Veled, J., 2005. Mechanisms of ENSO-forcing of hemispherically symmetric precipitation variability. *Quarterly Journal of the Royal Meteorological Society* 131, 1501–1527.
- Shackleton, N.J., 2000. The 100,000 year ice-age cycle identified and found to lag temperature, carbon dioxide and orbital eccentricity. *Science* 289, 1897–1902.
- Stott, L., Timmermann, A., Thunell, R., 2007. Southern hemisphere and deep-sea warming led deglacial atmospheric CO₂ rise and tropical warming. *Science* 318, 435–438.
- Stouffer, R.J., Yin, J., Gregory, J.M., Dixon, K.W., Spelman, M.J., Hurlin, W., Weaver, A. J., Eby, M., Flato, G.M., Hasumi, H., Hu, A., Jungclaus, J.H., Kamenkovich, I.V., Levermann, A., Montoya, M., Murakami, S., Nawrath, S., Oka, A., Peltier, W.R., Robitaille, D.Y., Sokolov, A., Vettoretti, G., Weber, S.L., 2006. Investigating the causes of the response of the thermohaline circulation to past and future climate changes. *Journal of Climate* 19, 1365–1387.
- Strelin, J.A., Malagnino, E.C., 2000. Late-glacial history of Lago Argentino, Argentina, and age of the Puerto Bandera moraines. *Quaternary Research* 54, 339–347.
- Sugden, D., 2005. Late-glacial glacier events in southernmost South America and their global significance. *Geografiska Annaler* 87, 271.

- Sugden, D., Bentley, M.J., Fogwill, C.J., Hulton, N.R.J., McCulloch, R.D., Purves, R.S., 2005. Late-Glacial glacier events southernmost South America: a blend of “northern” and “southern” hemispheric climatic signals? *Geografiska Annaler* 87A, 273–288.
- Thompson, D.W.J., Kennedy, J.J., Wallace, J.M., Jones, P.D., 2008. A large discontinuity in the mid-twentieth century in observed global-mean surface temperature. *Nature* 453, 646–649.
- Tovar, D.S., Shulmeister, J., Davies, T.R., 2008. Evidence for a landslide origin of New Zealand’s Waiho Loop moraine. *Nature Geoscience* 1, 524–526.
- Turney, C.S.M., Roberts, R.G., de Jonge, N., Prior, C., Wilmshurst, J.M., McGlone, M.S., Cooper, J., 2007. Redating the advance of the New Zealand Franz Josef Glacier during the last termination: evidence for asynchronous climate change. *Quaternary Science Reviews* 26, 3037–3042.
- Visser, K., Thunell, R., Stott, L., 2003. Magnitude and timing of temperature change in the Indo-Pacific warm pool during deglaciation. *Nature* 421, 152–155.
- Weaver, A.J., Saenko, O., Clark, P.U., Mitrovica, J.X., 2003. Meltwater pulse 1A from Antarctica as a trigger of the Bølling-Allerød warm interval. *Science* 299, 1709–1713.
- Weldeab, S., Schneider, R.R., Kölling, M., 2006. Deglacial sea surface temperature and salinity increase in the western tropical Atlantic in synchrony with high latitude climate instabilities. *Earth and Planetary Science Letters* 241, 699–706.
- Yancheva, G., Nowaczyk, N.R., Mingram, J., Dulski, P., Schettler, G., Negendank, J.F.W., Liu, J., Sigman, D.M., Peterson, L.C., Haug, G.H., 2007. Influence of the inter-tropical convergence zone on the East Asian monsoon. *Nature* 445, 74–77.
- Zhang, R., Delworth, T.L., 2005. Simulated tropical response to a substantial weakening of the Atlantic thermohaline circulation. *Journal of Climate* 18, 1853–1860.